Recent Results from the STAR Beam Energy Scan-II
- Selected with Bias

Guannan Xie

University of Chinese Academy of Sciences

Oct. 6, 2023

Contents

- Introduction
- STAR Experiment & BES-II
- Productions & Yields
- Collectivity & Criticality
- Correlations and EM etc
- Summary and Outlook

Exploring QCD Phase Diagram

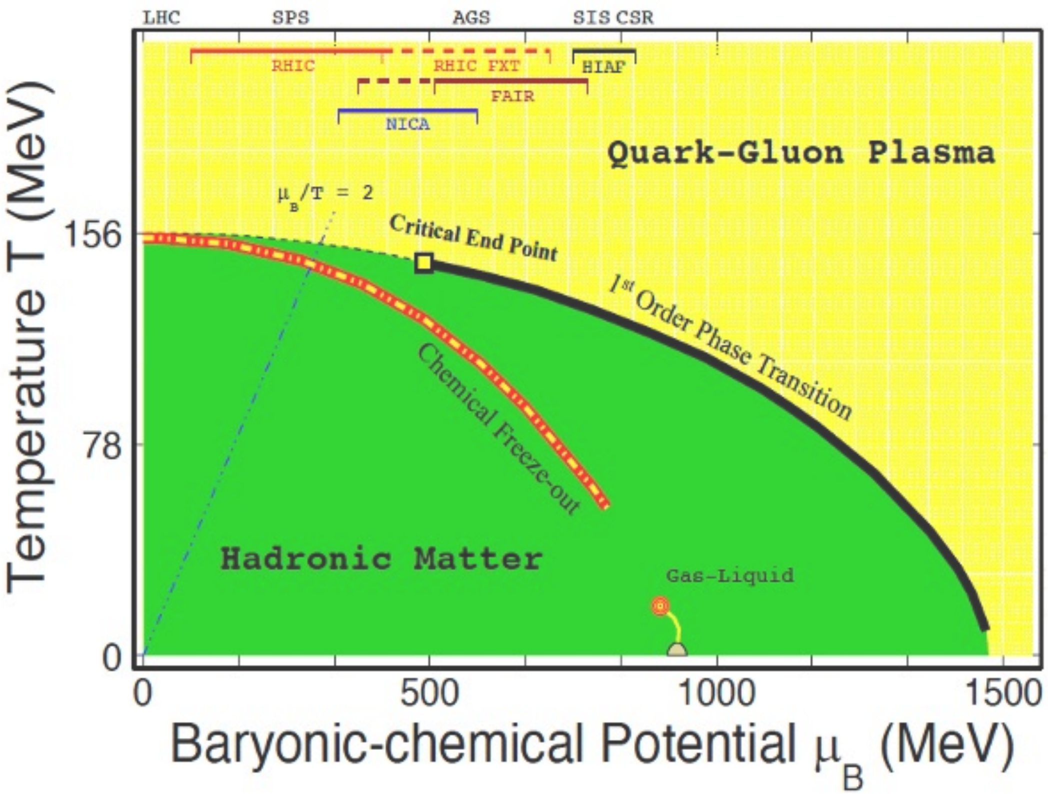

Conjectured phase diagram of strong interaction matter

- Study properties of the QCD matter
- Locate possible QCD phase boundary and Critical End Point

Particle production:

- Understand medium properties and different particle production mechanisms

Collective flow:

- Study properties of the produced medium, EoS

Correlations and Criticality:

- Critical Point

……

STAR Experimental

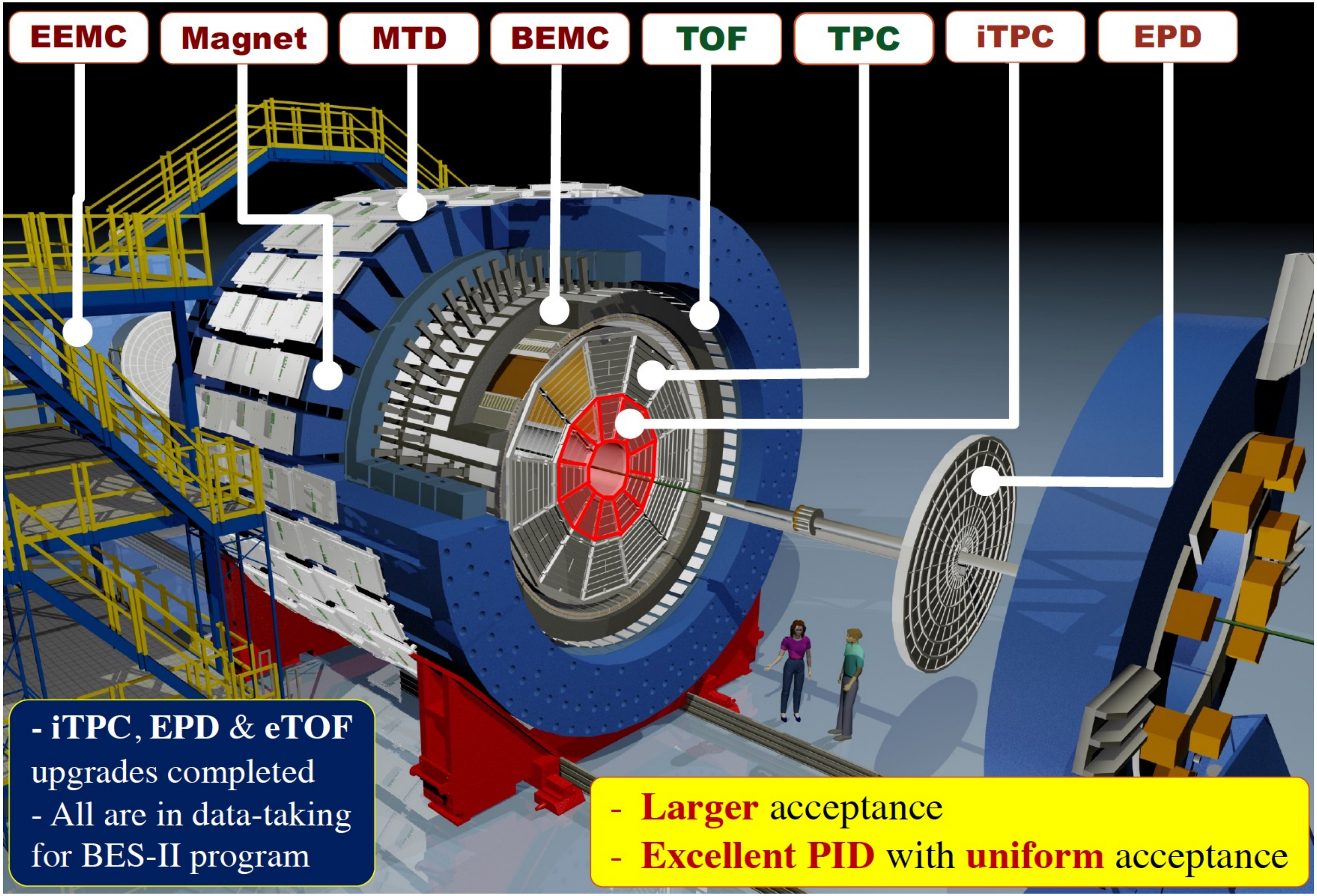

- iTPC, EPD & eTOF upgrades completed
- All are in data-taking for BES-II program

- **Larger** acceptance
- **Excellent PID** with **uniform** acceptance

FXT Setup @ STAR

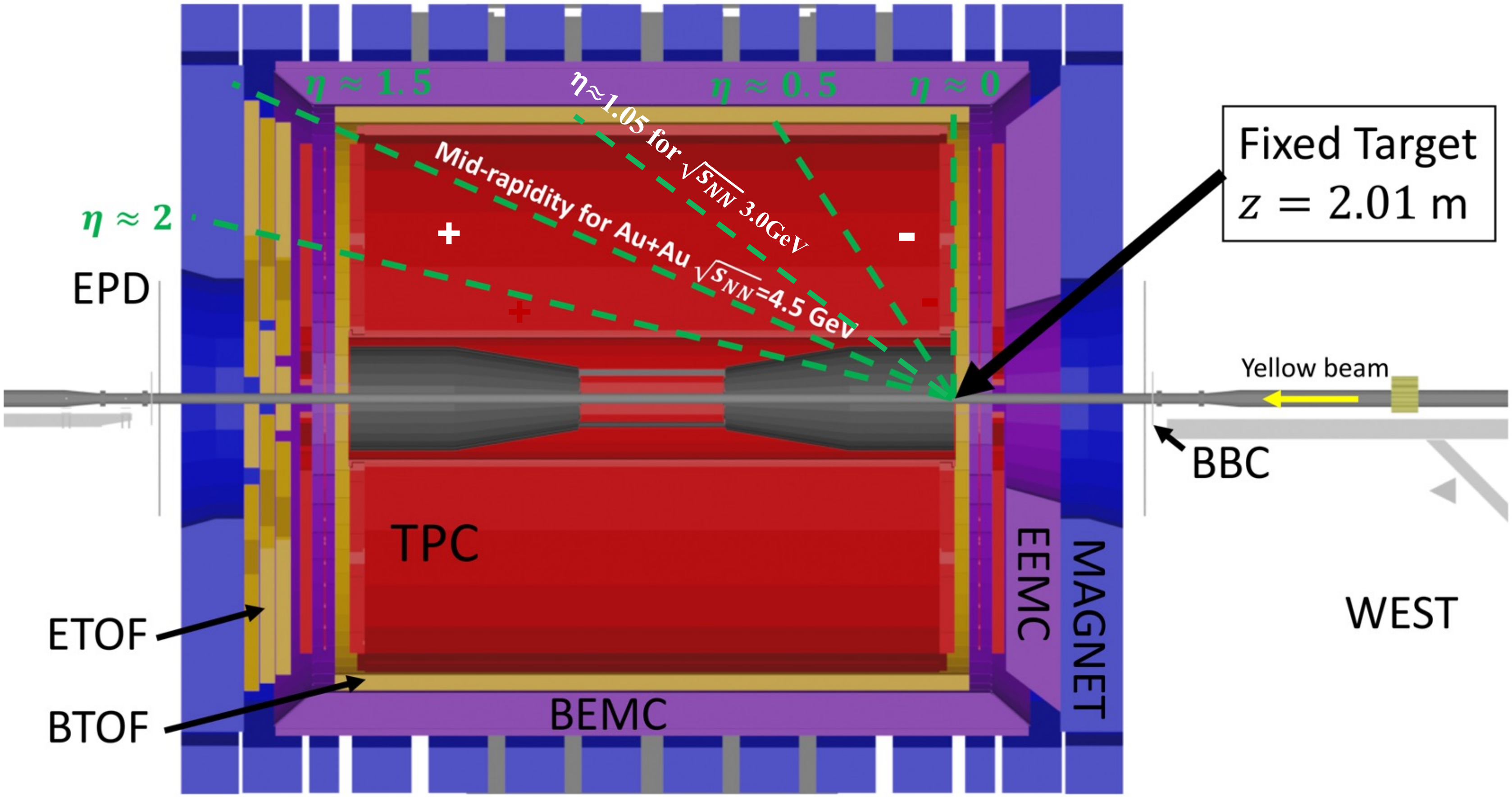

Good mid-rapidity coverage for STAR FXT 3 GeV (and up to 4.5GeV)

Conventions: beam-going direction is the positive direction

PID @ STAR FXT

TPC

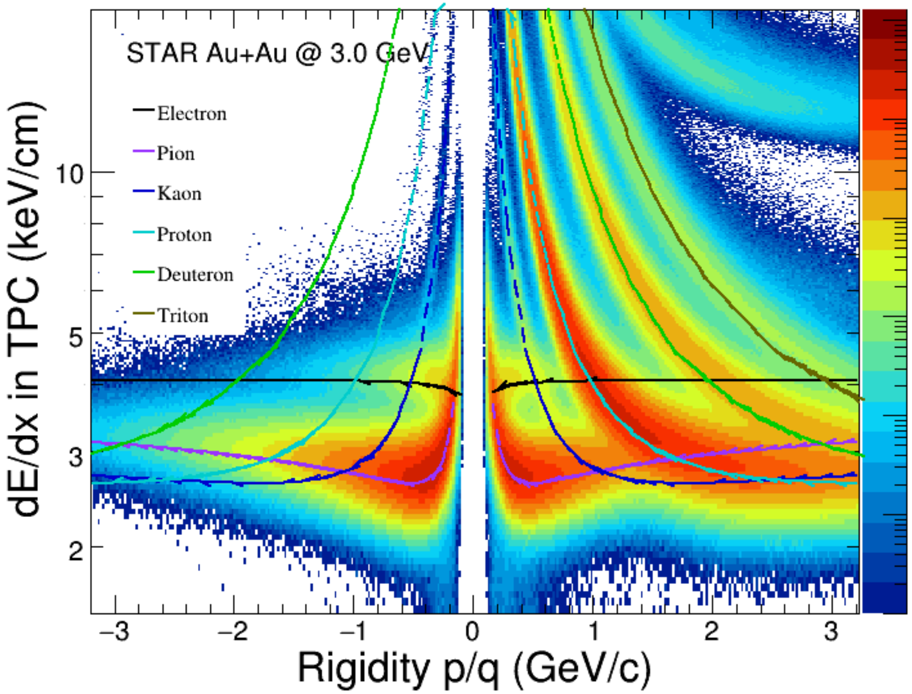

TOF

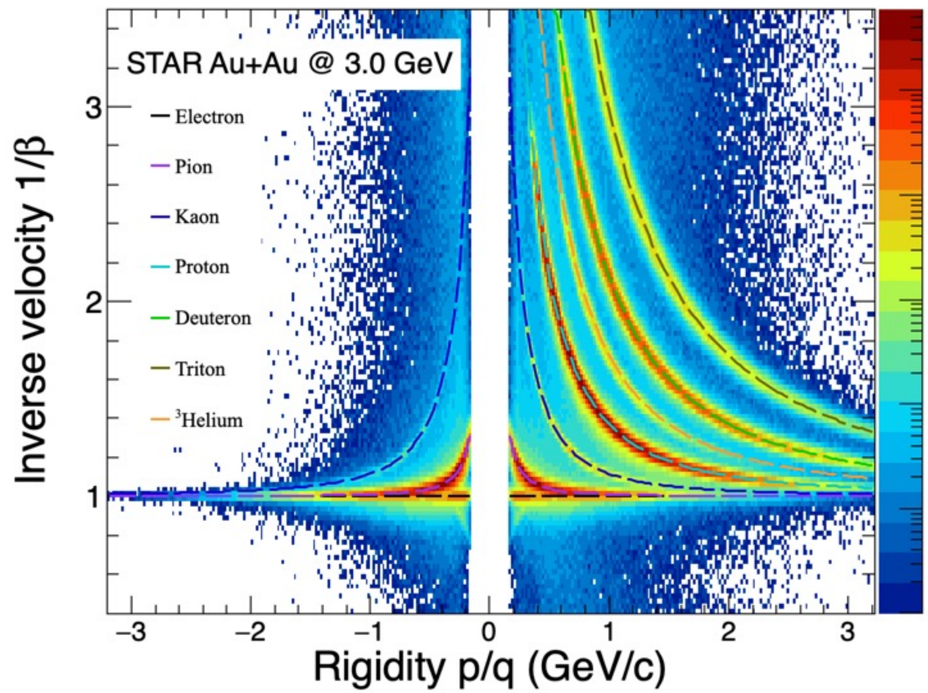

On average, “longer tracks” for FXT events than for collider events, better resolutions for both dE/dx and *1/β* in FXT mode

STAR Beam Energy Scan

Au+Au Collisions at RHIC											
Collider Runs						Fixed-Target Runs					
	$\sqrt{s_{NN}}$ (GeV)	#Events	μ_B	y_{beam}	run		$\sqrt{s_{NN}}$ (GeV)	#Events	μ_B	y_{beam}	run
1	200	380M	25MeV	5.3	r10,19	1	13.7(100)	50M	280MeV	-2.69	r21
2	62.4	46M	75MeV		r10	2	11.5(70)	50M	320MeV	-2.51	r21
3	54.4	1200M	85MeV		r17	3	9.2(44.5)	50M	370MeV	-2.28	r21
4	39	86M	112MeV		r10	4	7.7(31.2)	260M	420MeV	-2.1	r18,19,20
5	27	585M	156MeV	3.36	r11,18	5	7.2(26.5)	470M	440MeV	-2.02	r18,20
6	19.6	595M	206MeV	3.1	r11,19	6	6.2(19.5)	120M	490MeV	-1.87	r20
7	17.3	256M	230MeV		r21	7	5.2(13.5)	100M	540MeV	-1.68	r20
8	14.6	340M	262MeV		r14,19	8	4.5(9.8)	110M	590MeV	-1.52	r20
9	11.5	57M	316MeV		r10,20	9	3.9(7.3)	120M	633MeV	-1.37	r20
10	9.2	160M	372MeV		r10,20	10	3.5(5.75)	120M	670MeV	-1.2	r20
11	7.7	104M	420MeV		r21	11	3.2(4.59)	200M	699MeV	-1.13	r19
						12	3.0(3.85)	260+ 2000M	760MeV	-1.05	r18,20

Most Precise data to map the QCD phase diagram, $3 < \sqrt{s_{NN}} < 200\ GeV; 760 > \mu_B > 25\ MeV$;

Contents

Light Hadron Production

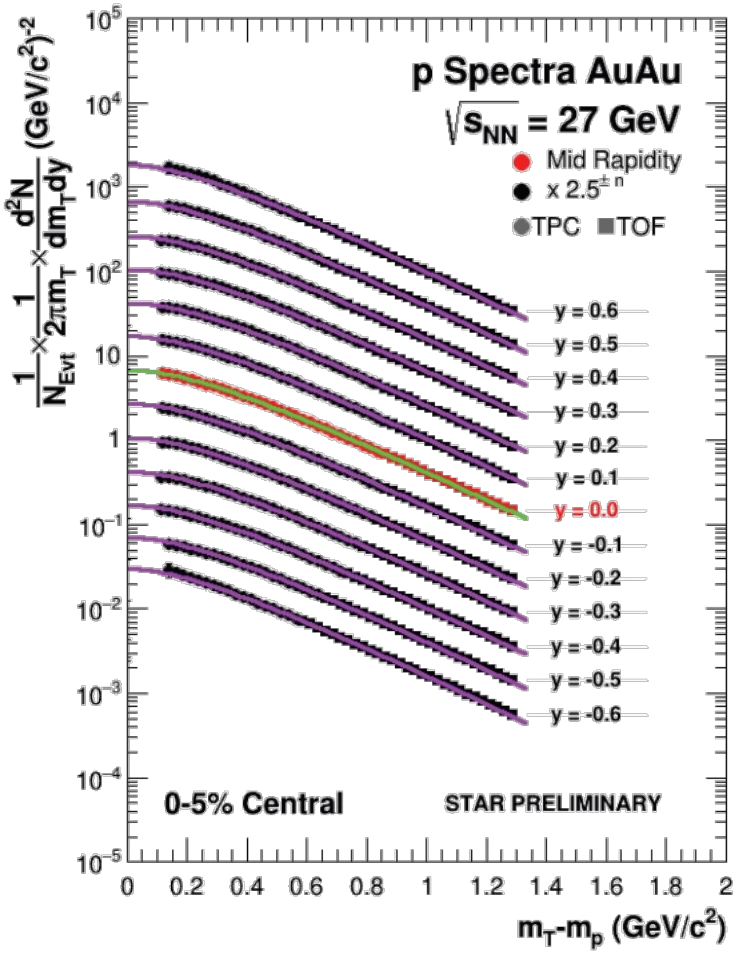

- Measure $\pi^{\pm}$, $K^{\pm}$, p, $\bar{p}$ across p_T and rapidity
- Kinetic & Chemical Freeze-out : μ_B and μ_S
  - Associated Production of K^+
  - Baryon Stopping
- Where are we on the QCD phase diagram at kinetic & chemical freeze-out?

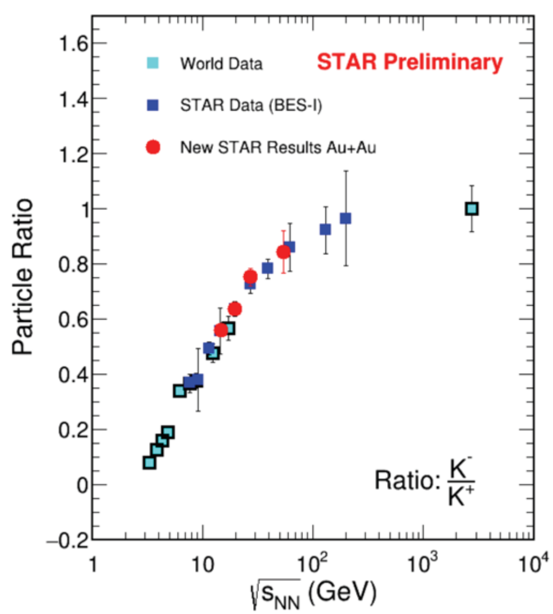

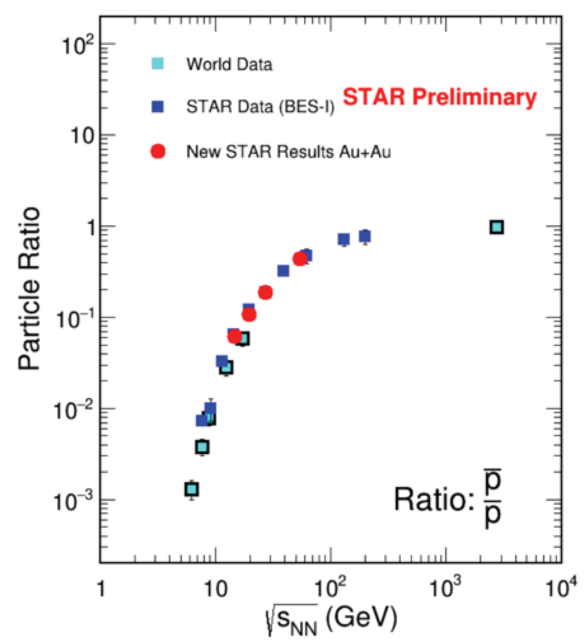

Light Hadron Production

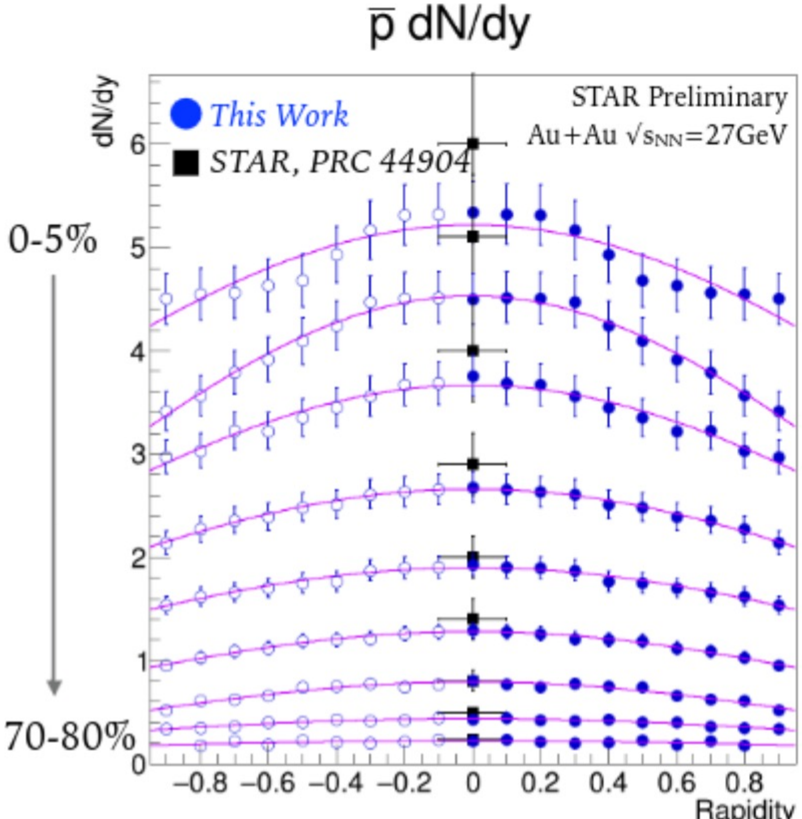

Feed-down corrected

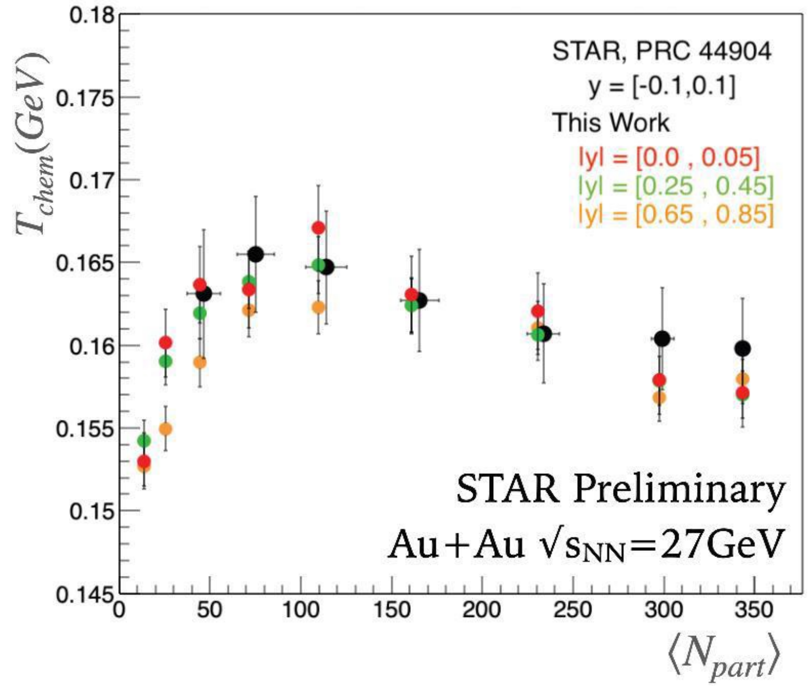

Fits by THERMUS
- Chemical equilibrium model

- High statistics of BES-II allows to make a rapidity dependence study of particle production
- With iTPC and eTOF upgrade more high precision data on particle production are on the way at lower energies

Chemical Freezeout Parameters

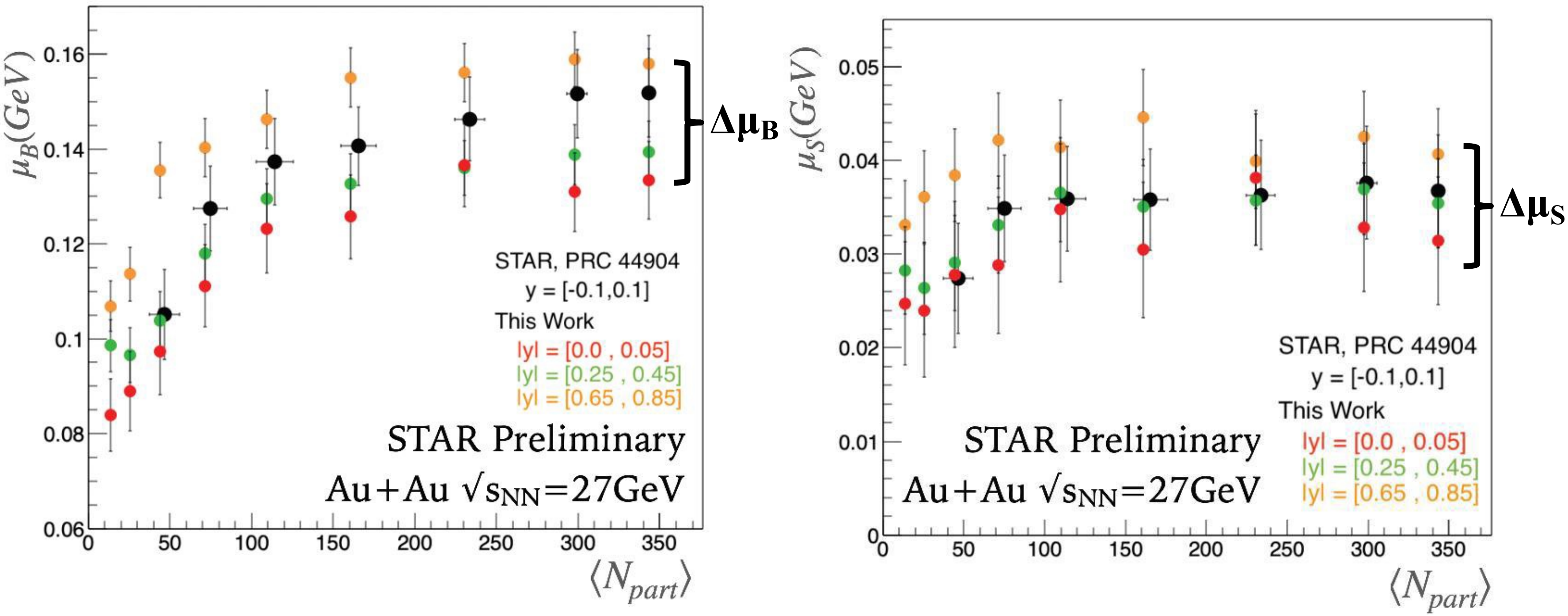

- Chemical equilibrium model
- $\Delta\mu_B \approx 25$ MeV for $\Delta y = 1$ at 27 GeV, $\Delta\mu_S \approx 10$ MeV for $\Delta y = 1$

- Similar rapidity dependence of the T_{chem} and μ_B, μ_S over particle multiplicity
- Precise study of the QCD phase diagram location of the interaction at different collision energies

Kinetic Freezeout Parameters

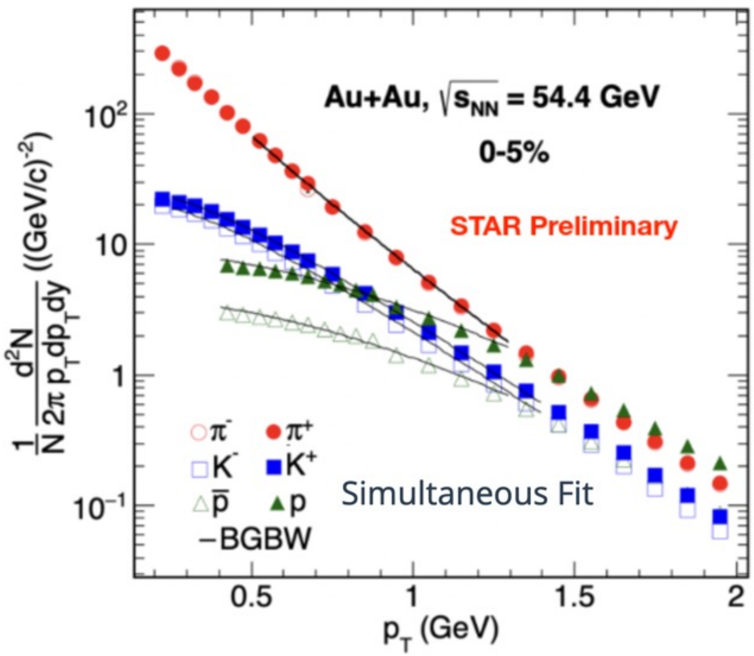

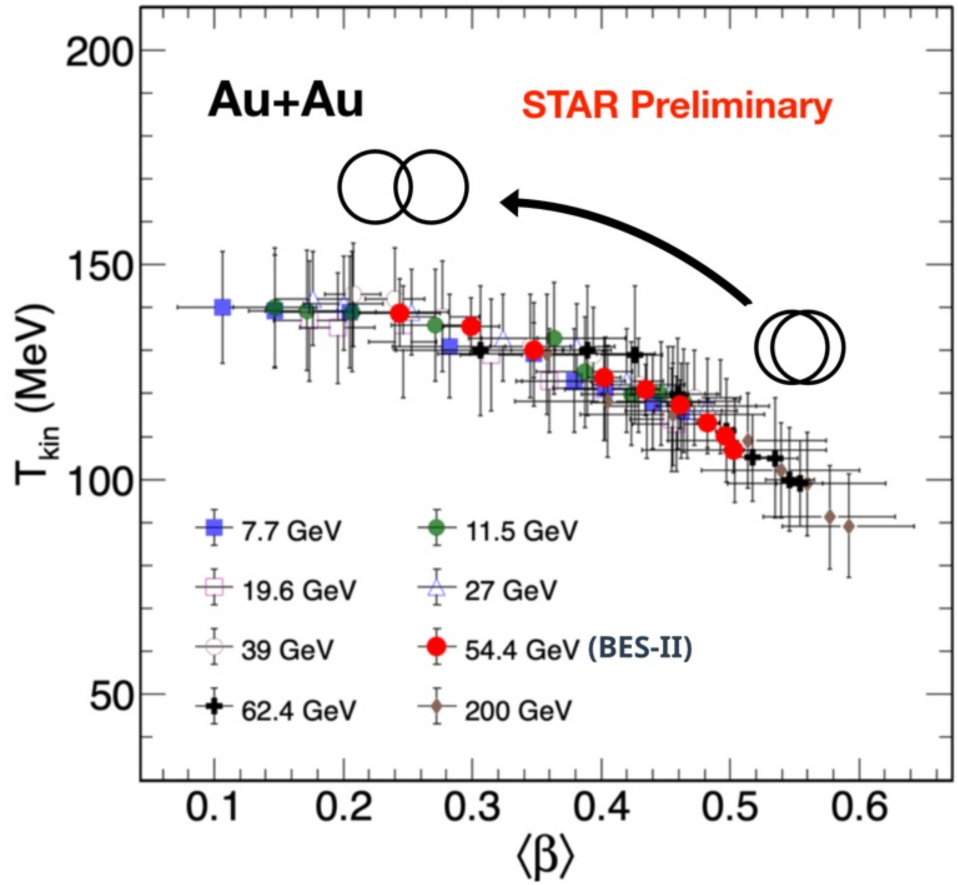

- Simultaneous fit with balst-wave

- T_{kin} and <β> show anti-correlated trend, similar to the other BES-I energies and with better precisions
- New dN/dy of $\pi^{\pm}$, $K^{\pm}$, p, $\bar{p}$ with p_T spectra @ $\sqrt{s_{NN}}$ = 14.6, 19.6, 27, 54.4 GeV

Nuclear modification factor

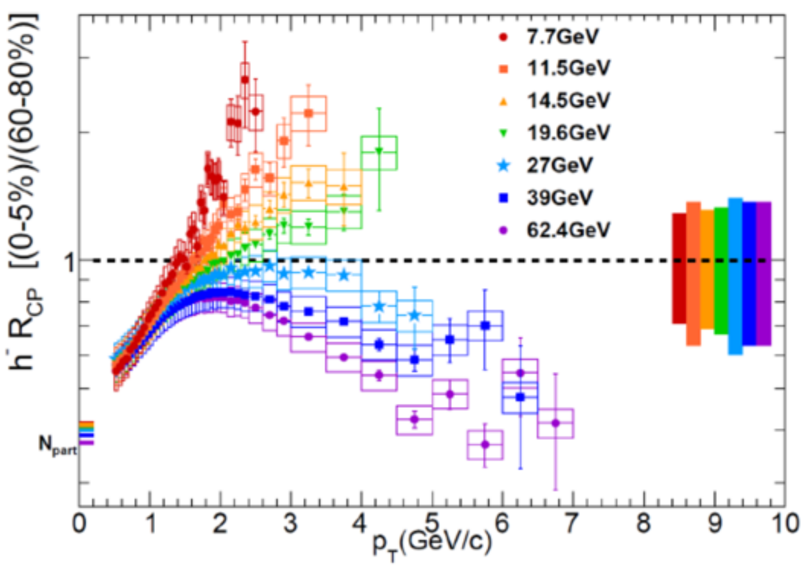

Phys. Rev. C 102 (2020) 34909
Phys. Rev. Lett. 121 (2018) 32301

$$R_{cp} = \frac{d^2 N dp_t d\eta / < N_{coll} > (central)}{d^2 N dp_t d\eta / < N_{coll} > (peripheral)}$$

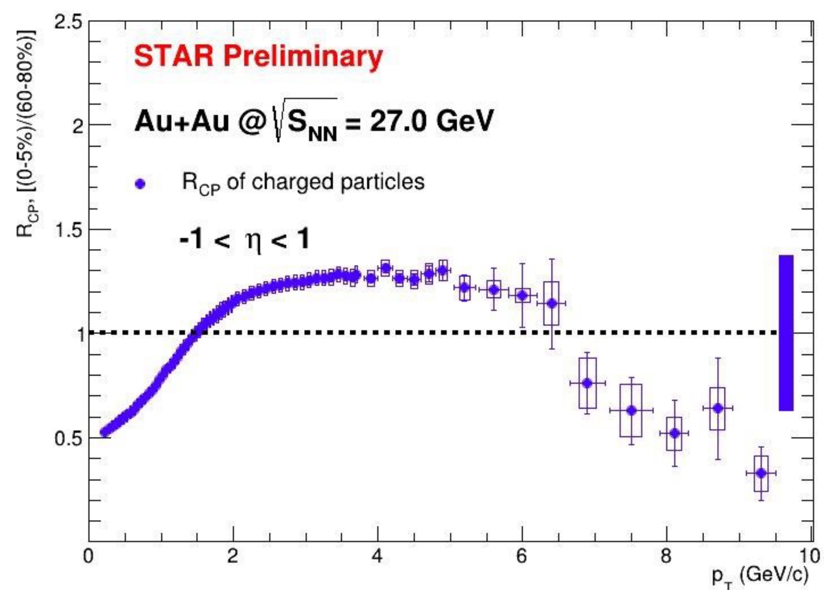

- R_{cp} has two regimes in the behavior depending on the collision energy:
- decrease of particle production with high p_T in central collisions at high energies
- smooth growth of particle production in central collisions at low collision energies.

High statistics of BES-II will allow to measure R_{cp} in high p_T region at low collision energies

Strangeness Productions

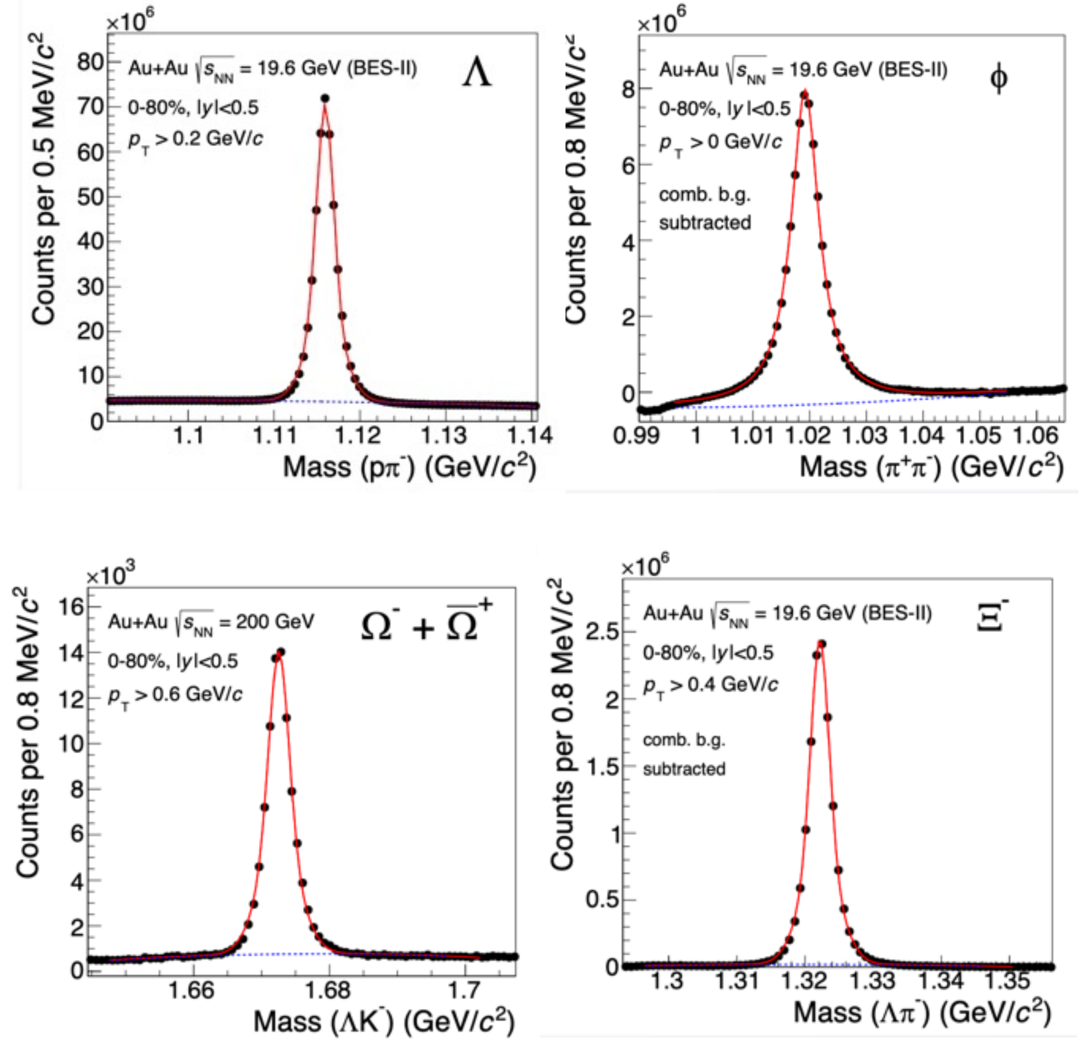

iTPC upgrade

$|\eta|$: 1.0 → 1.5

Improved dE/dx resolution

$\boldsymbol{p}_{\mathbf{T}}$ threshold: 120MeV → 60MeV

$$\mathrm{K_S^0} \rightarrow \pi^+ + \pi^- (\mathcal{B} = 69.2\%)$$
$$\Lambda(\bar{\Lambda}) \rightarrow p(\bar{p}) + \pi^-(\pi^+)(\mathcal{B} = 63.9\%)$$
$$\Xi^-\left(\bar{\Xi}^+\right) \rightarrow \Lambda(\bar{\Lambda}) + \pi^-(\pi^+)(\mathcal{B} = 99.9\%)$$
$$\Omega^-\left(\bar{\Omega}^+\right) \rightarrow \Lambda(\bar{\Lambda}) + K^-(K^+)(\mathcal{B} = 67.8\%)$$
$$\phi \rightarrow \mathrm{K}^+ + \mathrm{K}^- (\mathcal{B} = 49.1\%)$$

- Extend the measurements to low p_T and high rapidity

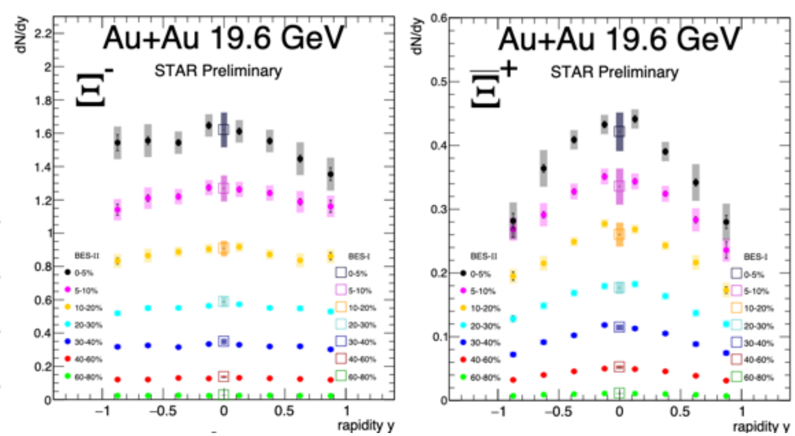

Strangeness Rcp & B/M Ratios

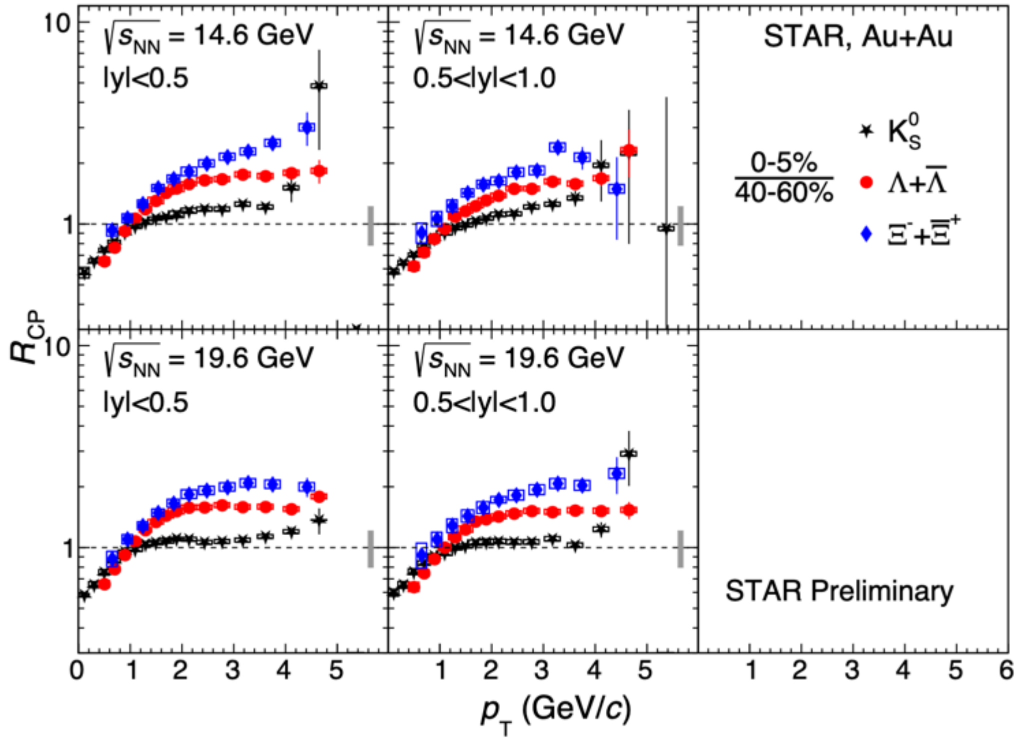

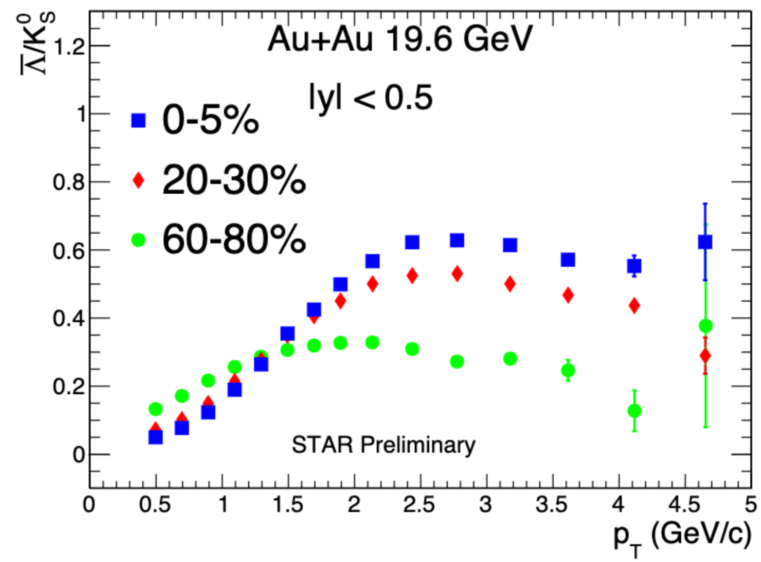

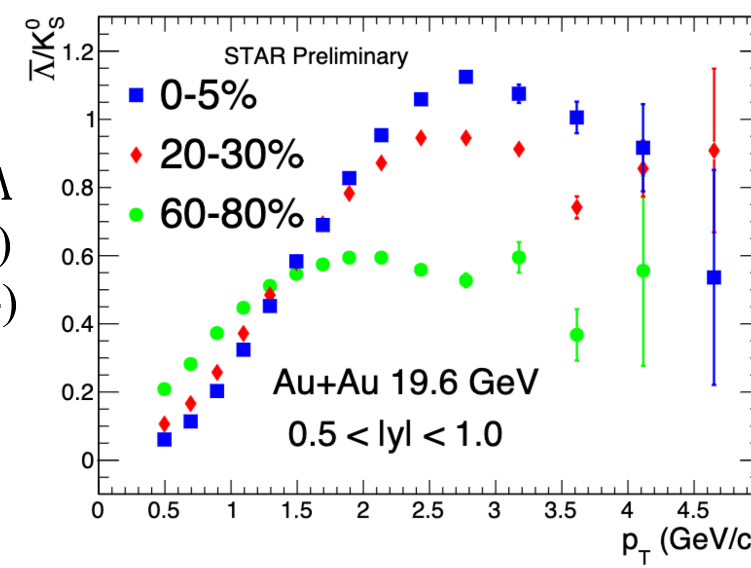

- The enhancement is stronger for Ξ^- compare to Λ and K_s^0 (a proposed signature for QGP formation)
- Clear centrality and rapidity dependence of (anti-) baryon-to-meson ratio at intermediate p_T.
- Baryon enhancement is observed in all measured rapidity regions with high precision

Light Nuclei & Hypernuclei

Nuclei are loosely bound objects with binding energies of few MeV
Hypernuclei are nuclei containing at least one hyperon
- N/Z + dimension on strangeness

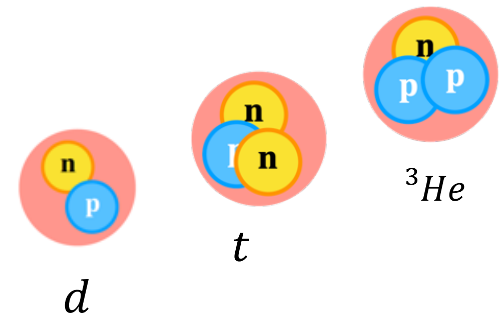

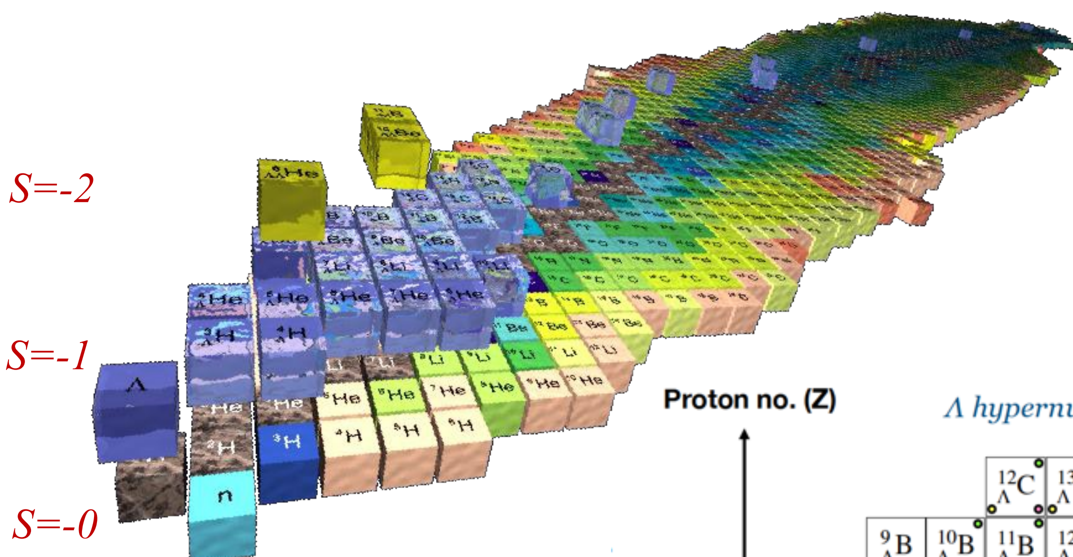

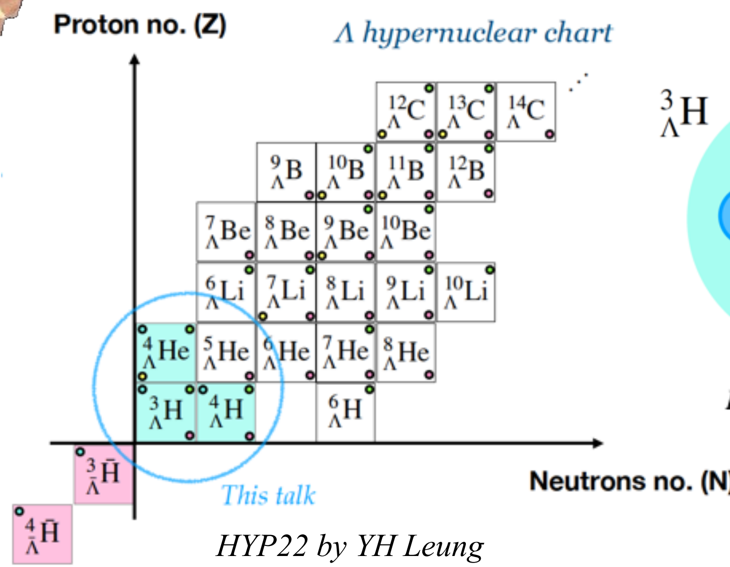

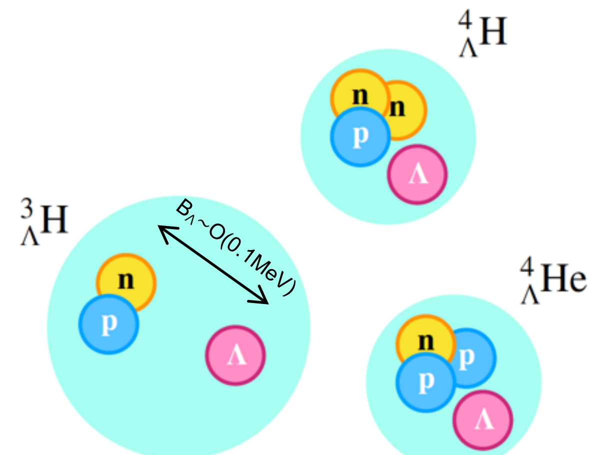

$B_\Lambda = (m_d + m_\Lambda - m_{^3_\Lambda H})c^2$

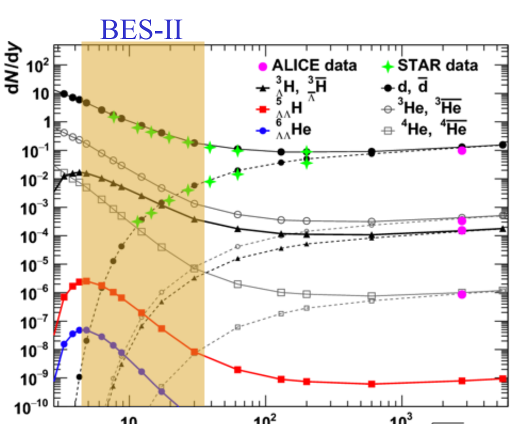

Light Nuclei & Hypernuclei (II)

Phys. Lett. B 684 (2010) 224
Phys. Lett. B 781 (2018) 499
Phys.Rev. Lett. 114, 092301 (2015)

1. What can (hyper)nuclei production in heavy-ion collisions tell us about the QCD phase diagram and the nuclear equation-of-state?

- Sensitive to critical fluctuations and the onset of deconfinement

$$\frac{t \times p}{d^2}$$

Sensitive to neutron density fluctuations

$$\frac{{}^{3}_{\Lambda}\mathrm{H}}{{}^{3}\mathrm{He} \times \frac{\Lambda}{p}}$$

Sensitive to baryon-strangeness correlations

2. What is the role of hyperon-nucleon (YN) and hyperon-hyperon (YY) interaction in the equation-of-state of high baryon density matter

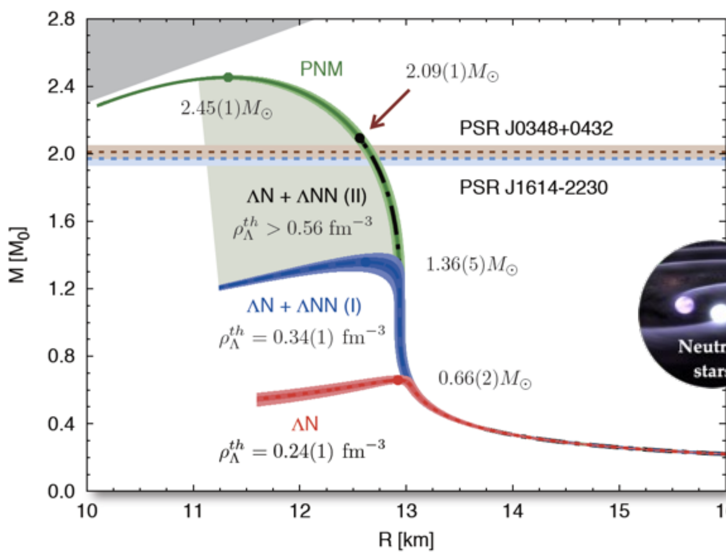

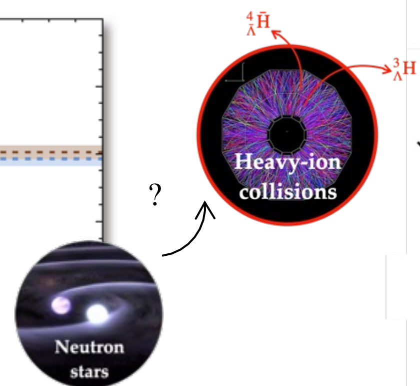

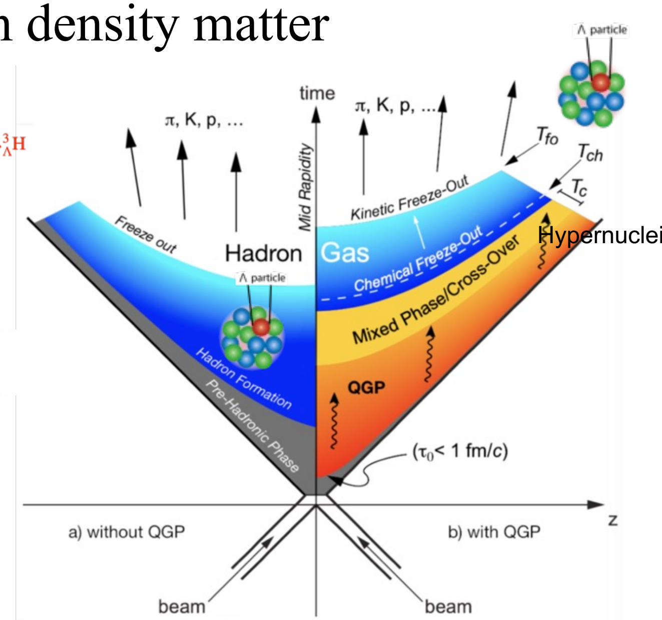

- Hyperon Puzzle: difficulty to reconcile the measured masses of neutron stars with the presence of hyperons in their interiors

When are hypernuclei formed? At freezeout? Or in medium?

Hypernuclei Reconstruction @ BES-II

$^{3}_{\Lambda}H \rightarrow\ ^{3}He\ \pi^{+}$

Phys. Rev. Lett. 128 (2022) 20, 202301
Y. Ji. STAR, QM 2023

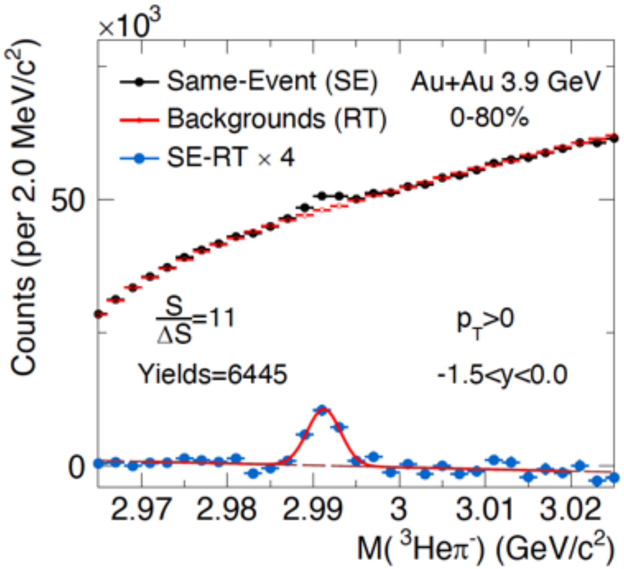

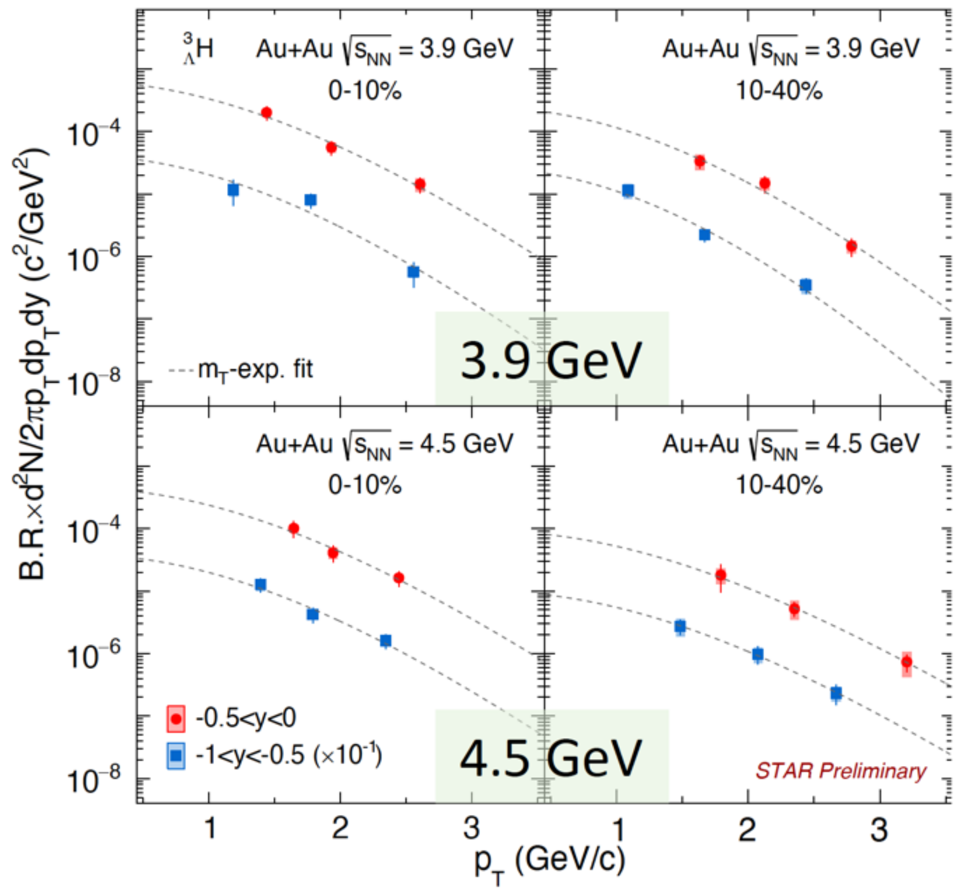

- New hypertriton results from 3.2, 3.5, 3.9, 4.5,7.7,14.6 GeV

Hypernuclei Yield vs. $\sqrt{s_{NN}}$

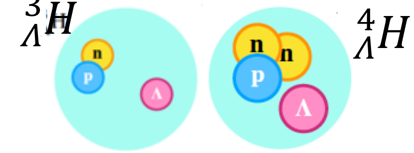

Phys. Rev. Lett. 128 (2022) 20, 202301

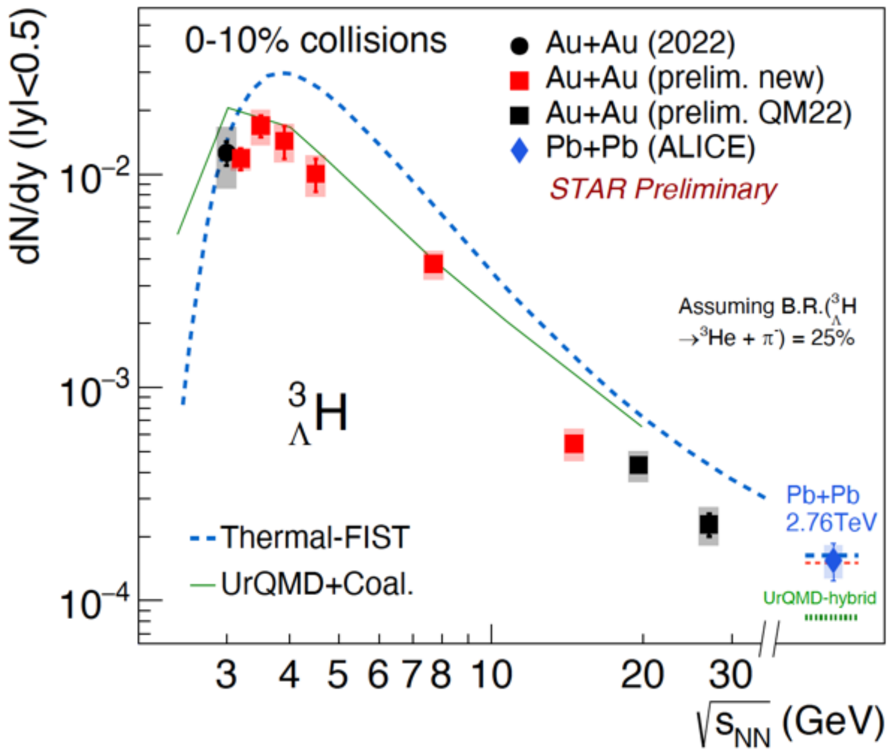

First energy dependence of hypernuclei production yields in high baryon region

Enhanced hypernuclei production at RHIC BES II w.r.t LHC due to increased baryon density at low energies.

Hadronic transport + coalescence models qualitatively describe the data.

Both hypertriton and triton yields are not fixed at chemical freeze-out (disfavor thermal), likely fixed at a later stage (coal.)

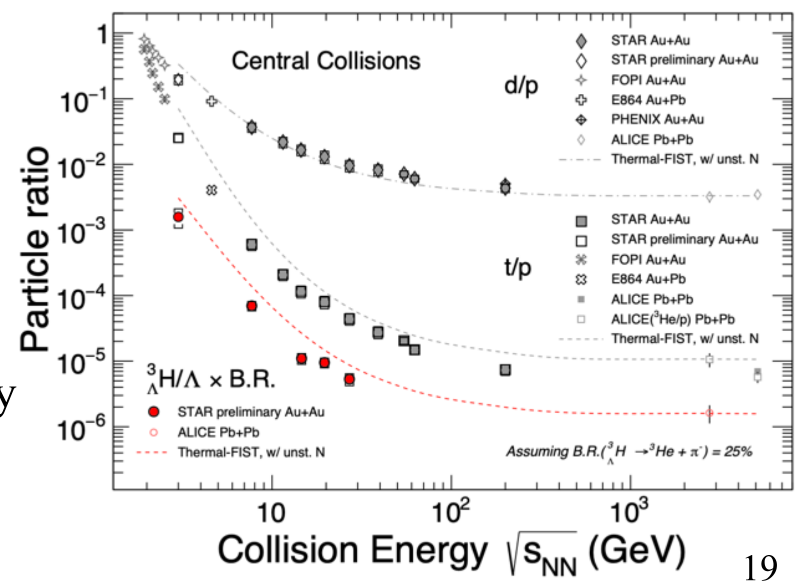

Strangeness Population Factor vs. $\sqrt{s_{NN}}$

Phys. Lett. B 684 (2010) 224

Increasing trend of S_3 originally proposed as a signature of onset of deconfinement

$$S_3 = \frac{{}^{3}_{\Lambda}H}{{}^{3}He \times \frac{\Lambda}{p}}$$

: removes the absolute difference of Λ/B yields versus beam energy.

- Data shows a hint of an increasing trend

- Coalescence + transport also suggest increasing trend – ${}^{3}_{\Lambda}H$ suppression due to large size

Phys. Rev. C 107 (2023) 1, 014912
Phys. Let. B 809 (2020) 135746

- Thermal-FIST also suggest increasing trend : unstable nuclei breakup ${}^{4}Li \rightarrow {}^{3}He\ p$

$$S_2 = \frac{{}^{3}_{\Lambda}H}{\Lambda \times d}$$

: recently s_2 also proposed as a sensitive probe

Chin. Phys. C 44, 11 (2020) 114001

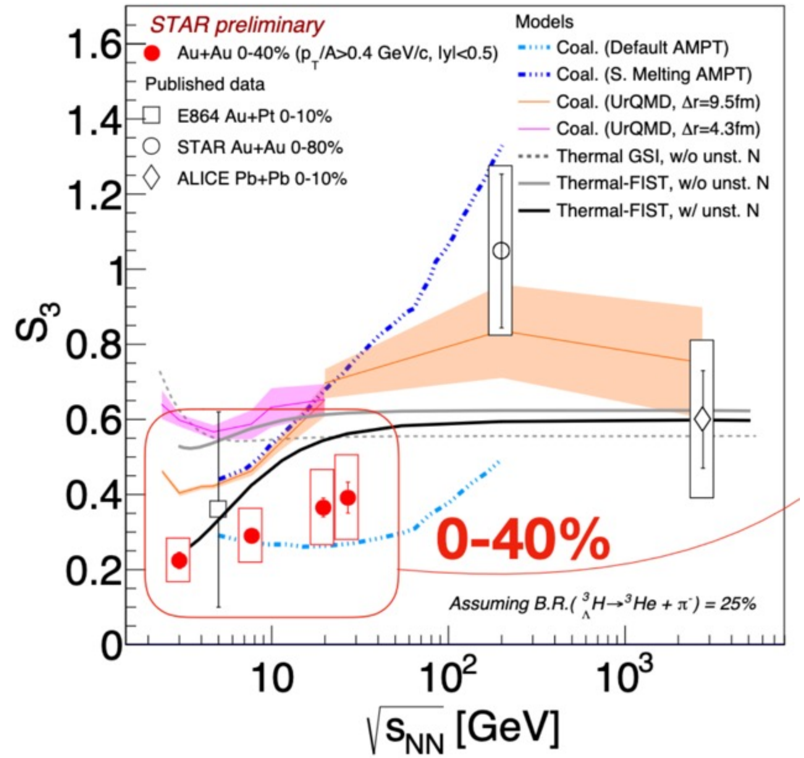

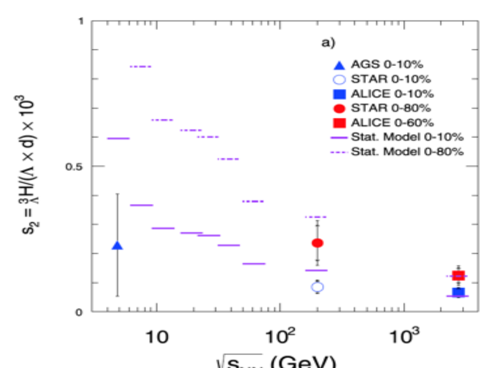

Guannan Xie

Note: For 19.6 and 27 GeV, take $^{3}He/t = 0.93 \pm 0.07$

Contents

Anisotropic Flow of Identified Particles

Z. Liu. STAR, QM 2023

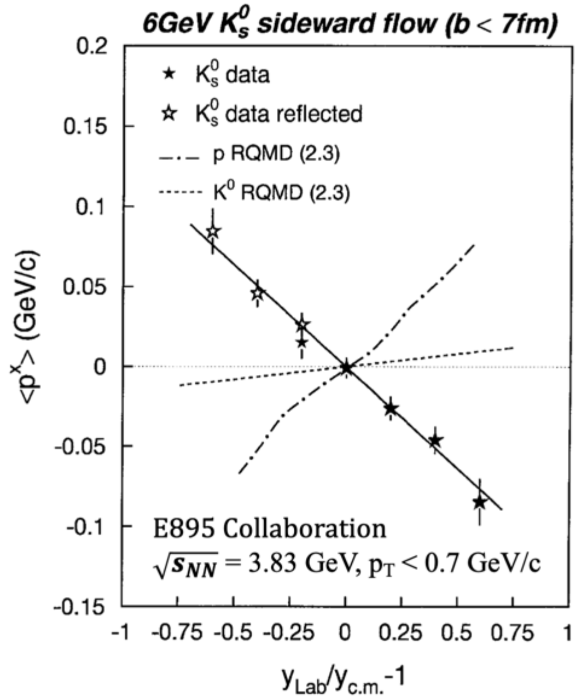

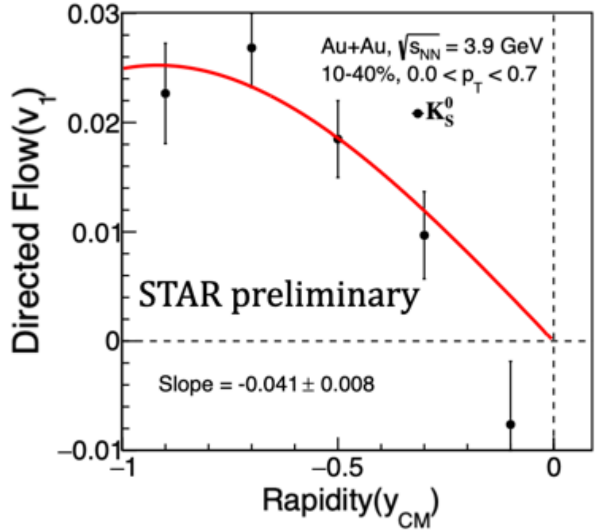

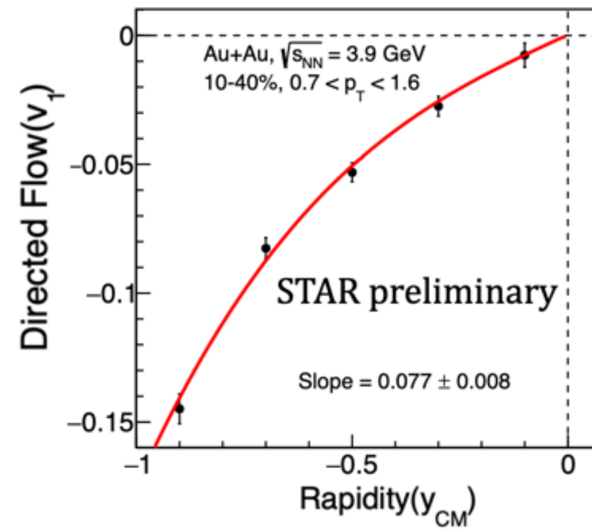

- E895: anti-flow of kaon at low p_T. Kaon potential ?
- 3.9 GeV: anti-flow observed for K_s^0 at $p_T < 0.7$ GeV/c.
- Positive flow of K_s^0 at $p_T > 0.7$ GeV/c.
- Strong p_T dependence of K_s^0 v1 slope

Anisotropic Flow of Identified Particles

Z. Liu. STAR, QM 2023

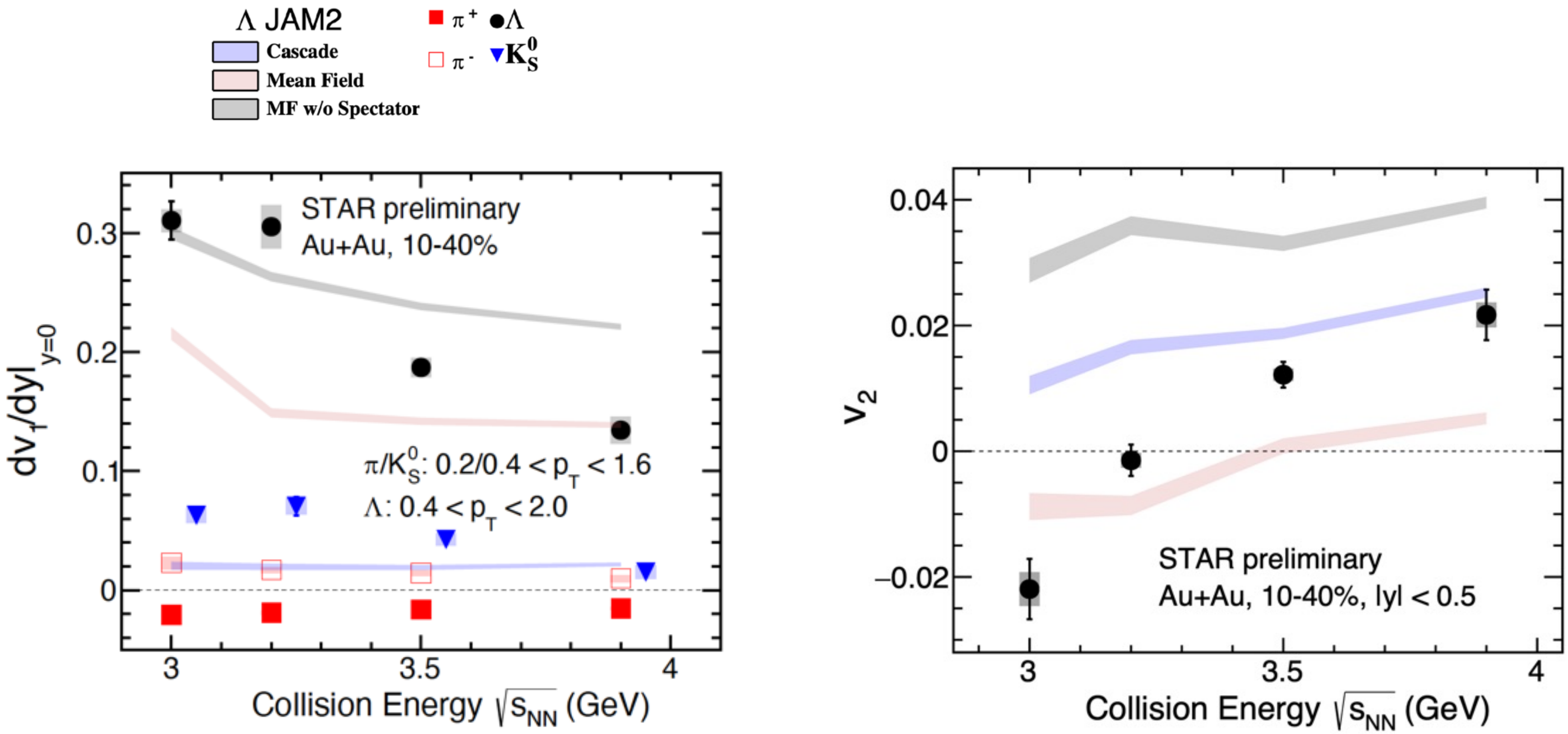

- v_1 slope decreases in magnitude as collider energy increases. -> Stronger tilted expansion
- Anti-flow could be explained by shadowing effect from spectator.

- Negative v_2 turns to positive: Out-of-plane flow (spectator effect) -> in-plane flow
- Mean-field and spectator shadowing play important role

NCQ scaling of Anisotropic Flow

Z. Liu. STAR, QM 2023

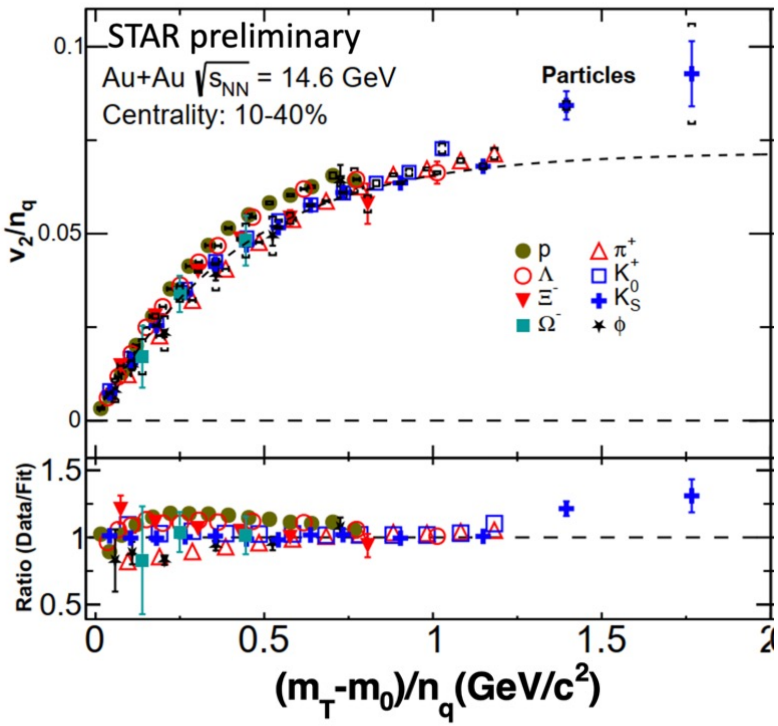

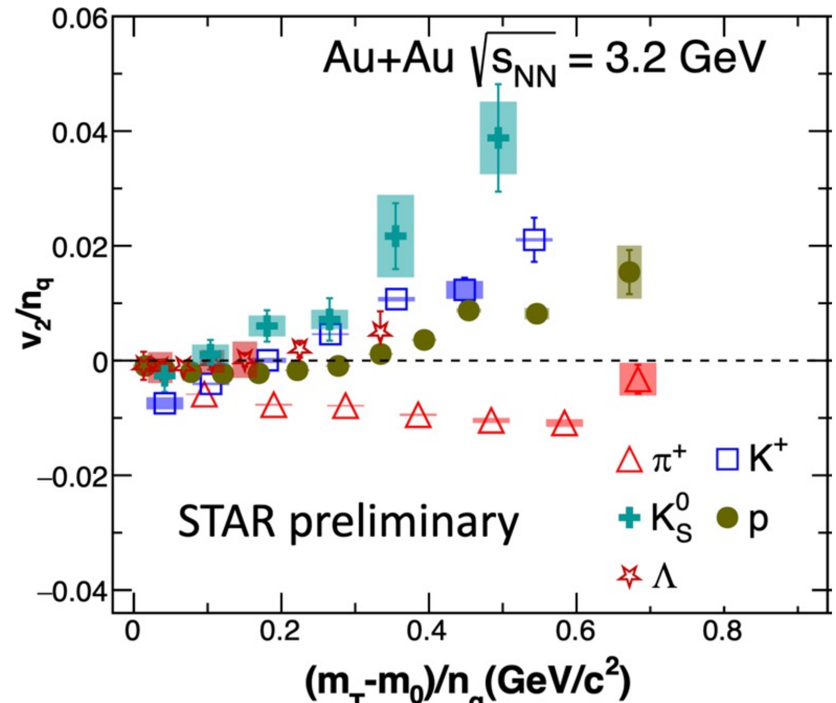

- NCQ scaling of v2 holds within uncertainties. Partonic interaction plays important role at 14.6 GeV
- NCQ scaling of v2 breaks completely at 3.2 GeV. -> Disappearing of partonic collectivity
- NCQ scaling violation at 3.2GeV and below : Partonic -> Hadronic

Light and HyperNuclei Collectivity

C. Han. STAR, QM 2023

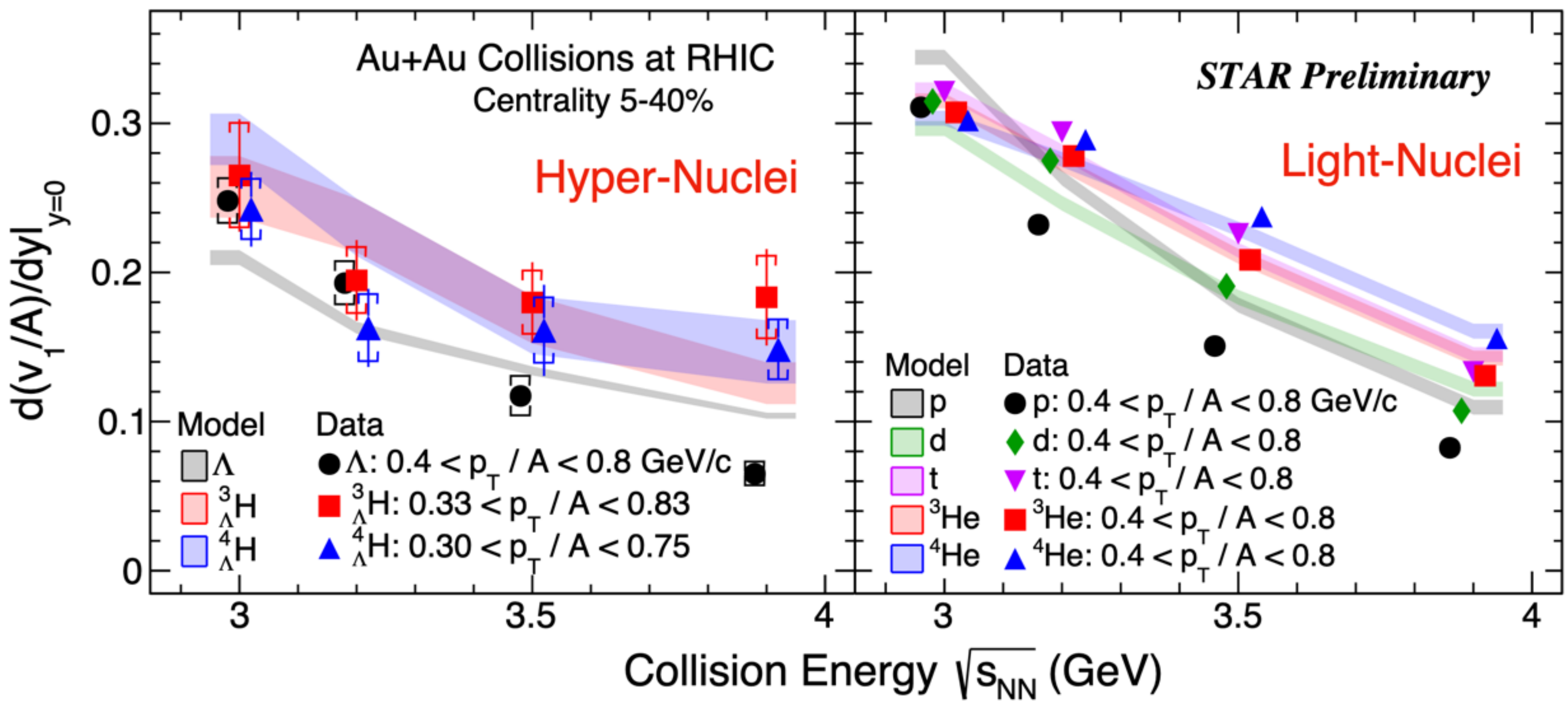

- Hypernuclei at high μ_B can probe Y-N (hyperon-nucleon) interactions
- Useful for neutron stars!
- v_1: Consistent w/Hadronic transport model
- Decreases with increasing collision energy

Particle Mass Dependence

C. Han. STAR, QM 2023

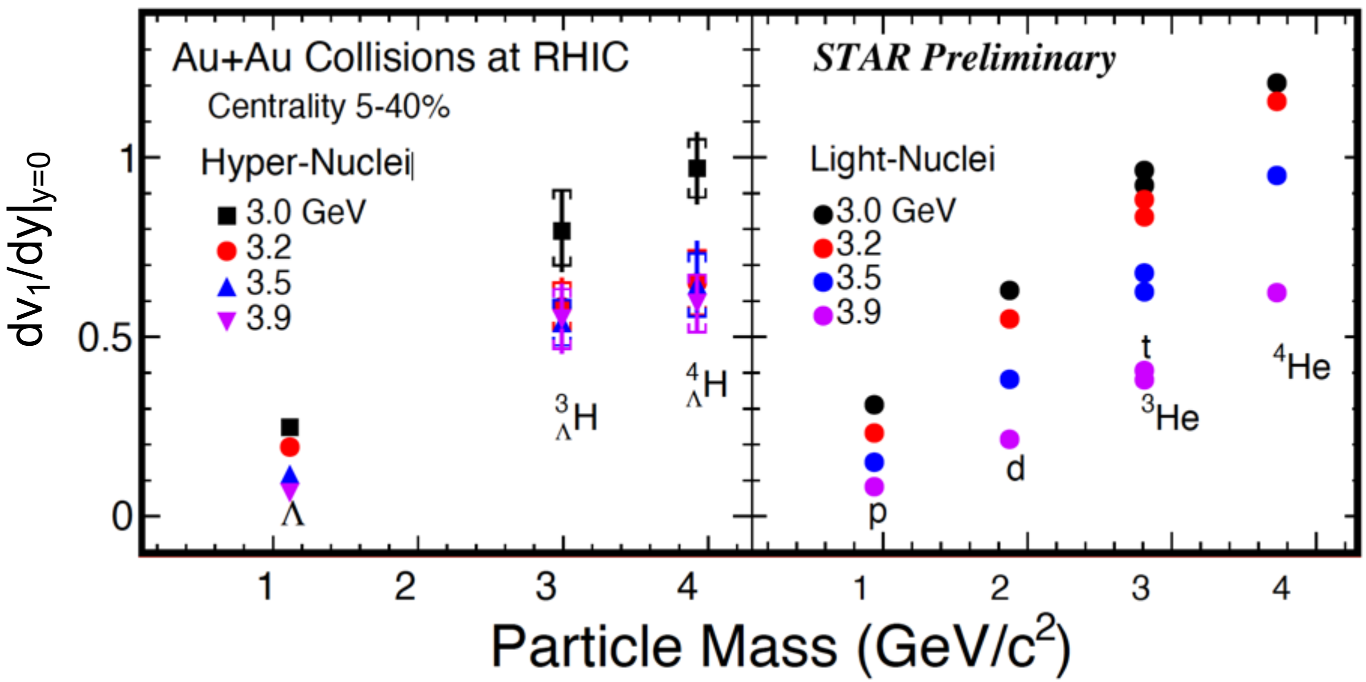

- The slopes of mid-rapidity v_1 for both light- and hyper-nuclei are scaled with A and/or mass
  - Across multiple collision energies
  - Coalescence mechanism may dominate

Elliptic and Triangular flow of Light Nuclei

R. Sharma. STAR. QM 2023

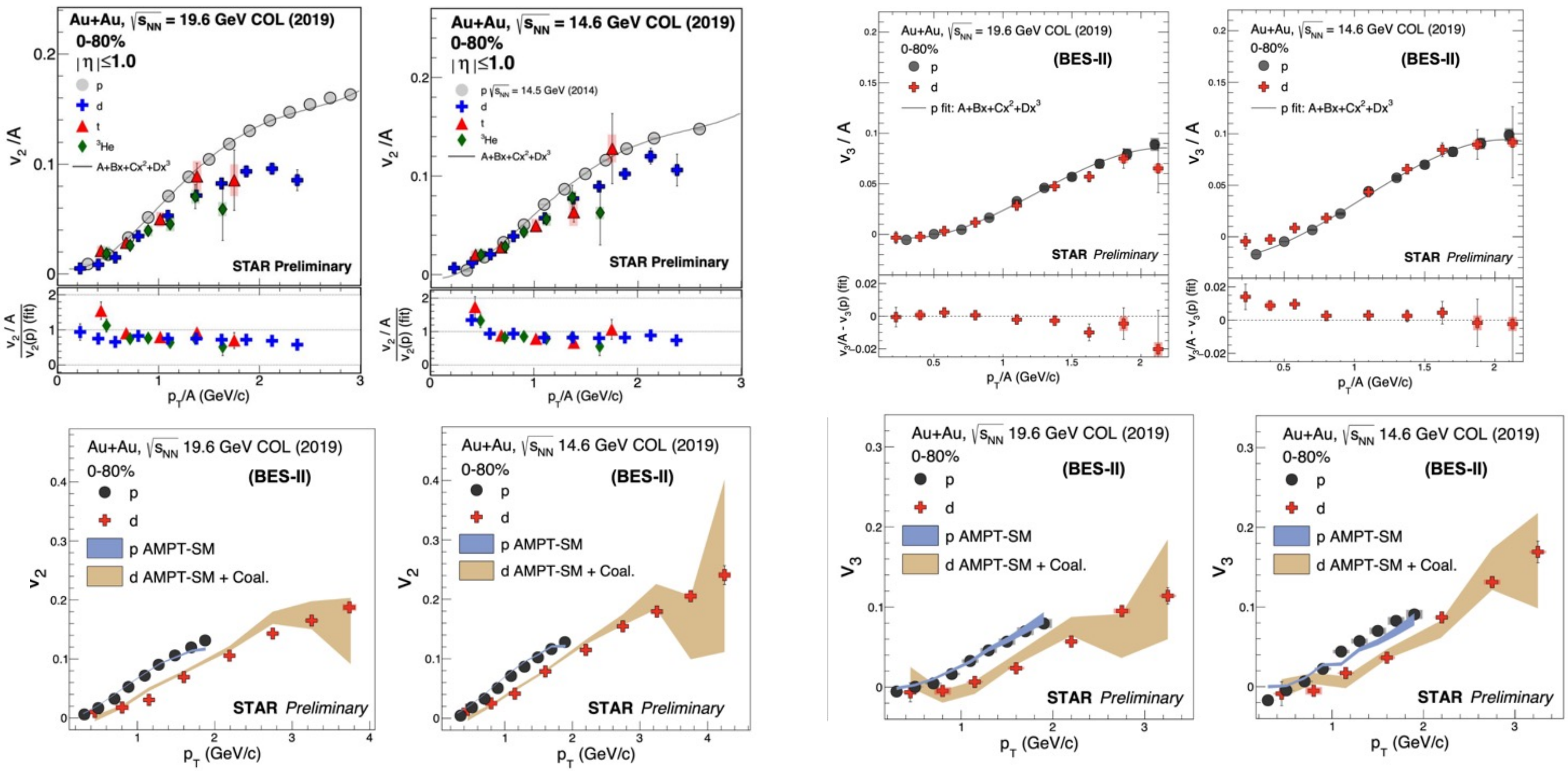

- Scaling for light nuclei species for v_2/A (~20-30%%) and for v_3/A (~10%) taking into account mass number of the nuclei was calculated
- AMPT+Coal. describes proton and deuteron v_2 and v_3
- Elliptic and Triangular flow measurements suggest coalescence to be the dominant mechanism of light nuclei production in heavy-ion collisions

Flow at High (Pseudo)Rapidity

X. Liu, STAR, QM 2023

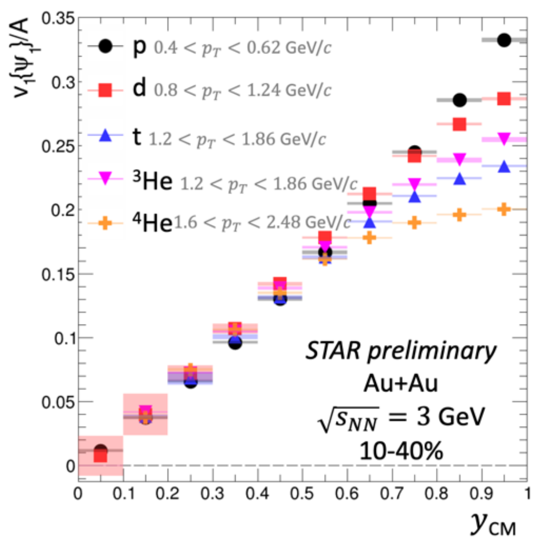

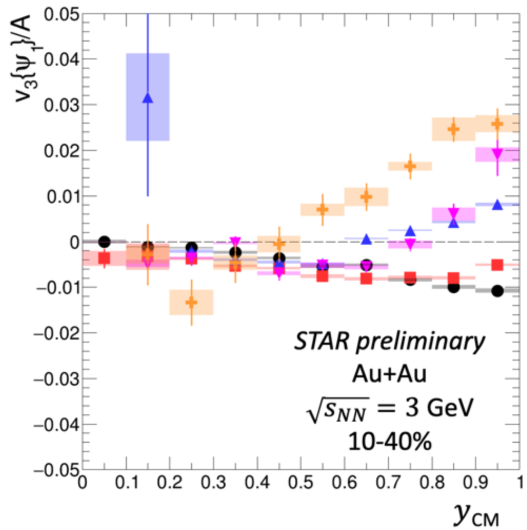

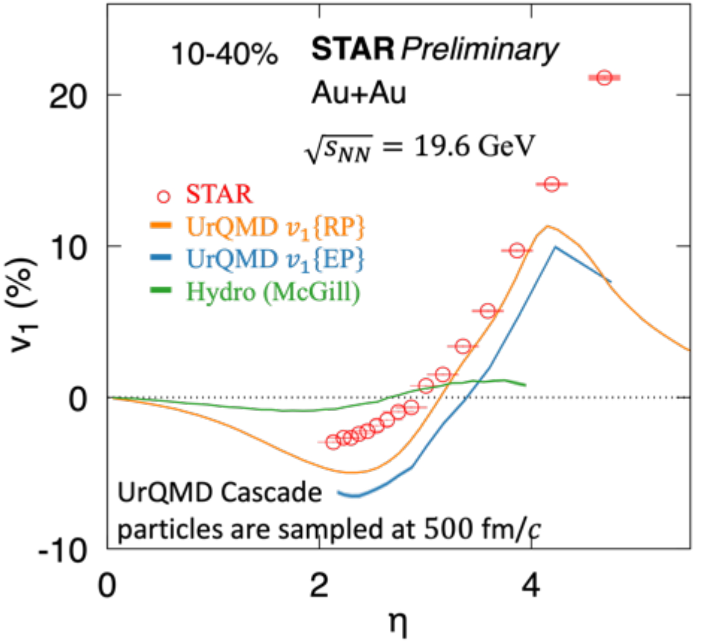

- Scaling for light nuclei species for v_1/A and for v_3/A
  - A-scaling holds below $y_{cm}<0.5$ (coalescence)
  - A-scaling breaks at $y_{cm}>0.5$ (fragments)
- Model comparisons suggest that nuclei fragments contribute significantly to $v1$ at large $|\eta|$ (may use to constrain the shear viscosity)

Fluctuation & CP Search

Phys. Rev. Lett. 130 (2023) 202301, *PRL* 128 (2022) 202302

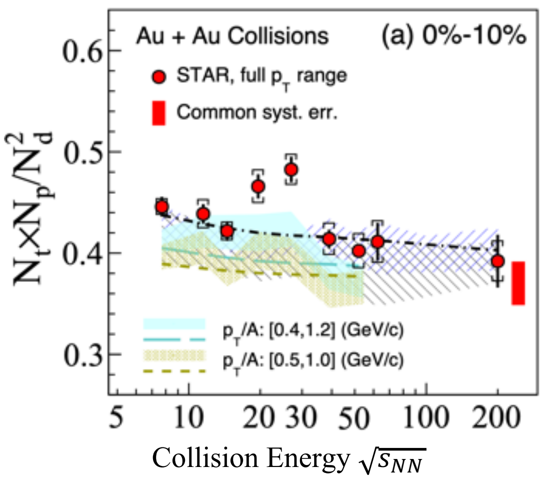

$$\frac{t \times p}{d^2} = g(1 + \Delta n)$$

In central collisions, non-monotonic behavior found in the light nuclei and net-proton fluctuations.
These 2 results will be released directly to paper, work in prog.

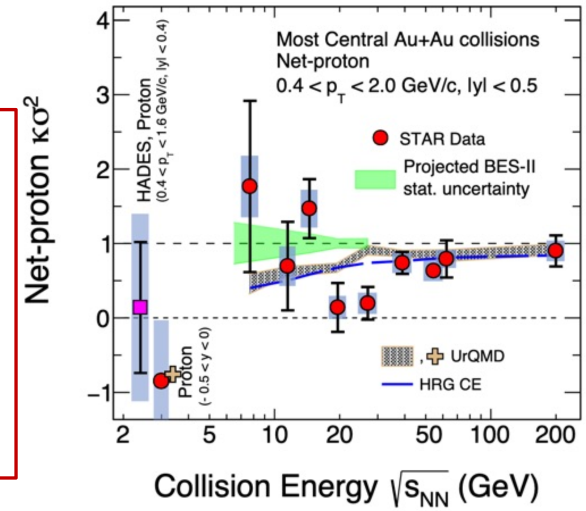

- Cumulant ratios directly related to susceptibilities
- Violation of ordering found at fixed target 3 GeV
- Reproduced by UrQMD at 3 GeV -> Suggests hadronic matter

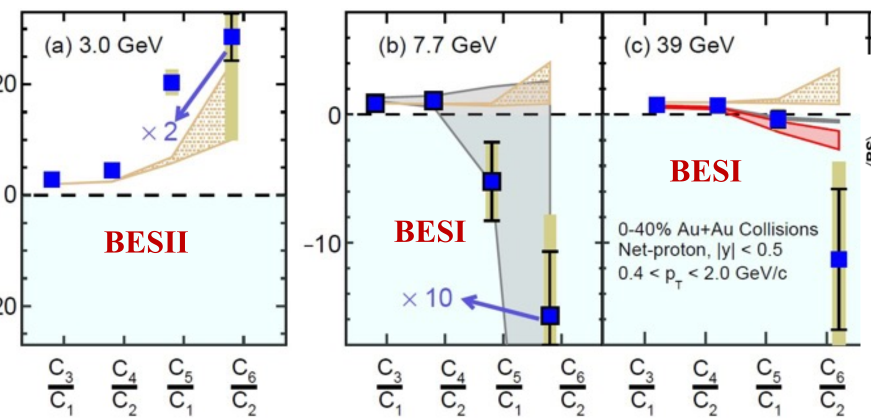

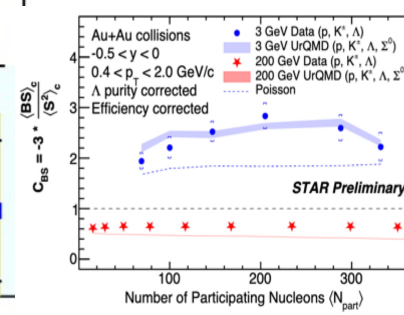

Contents

Correlations of $\pi\pi$, p-Λ, d-Λ

Y. Hu, STAR, QM 2023

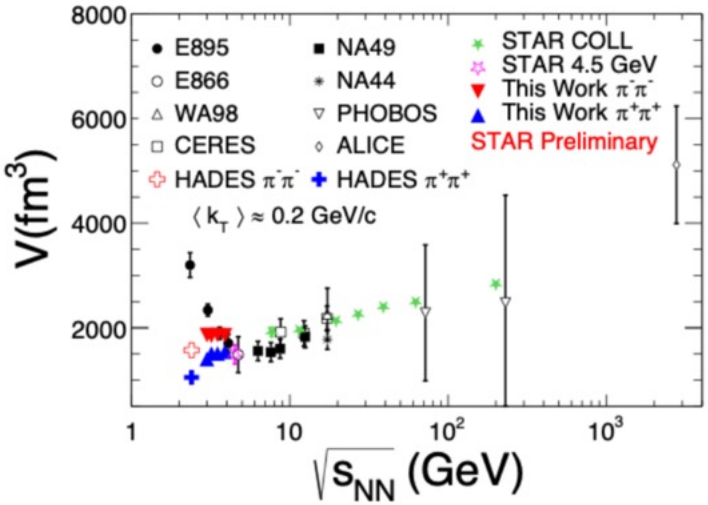

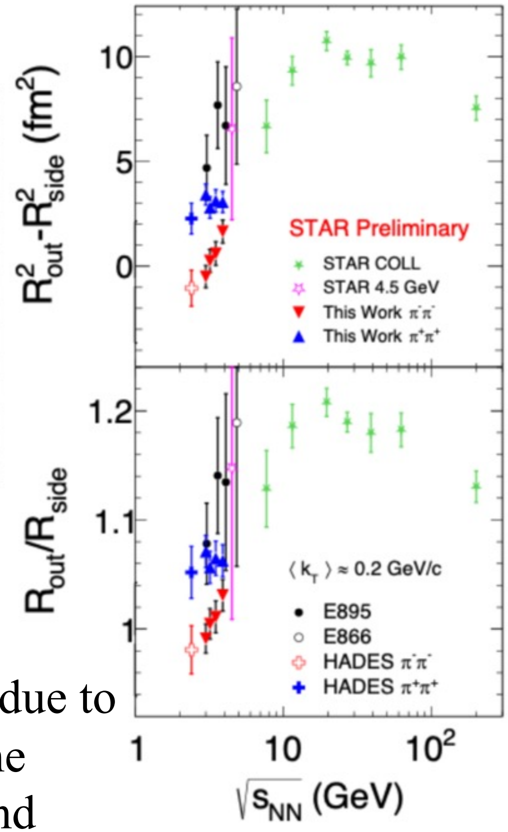

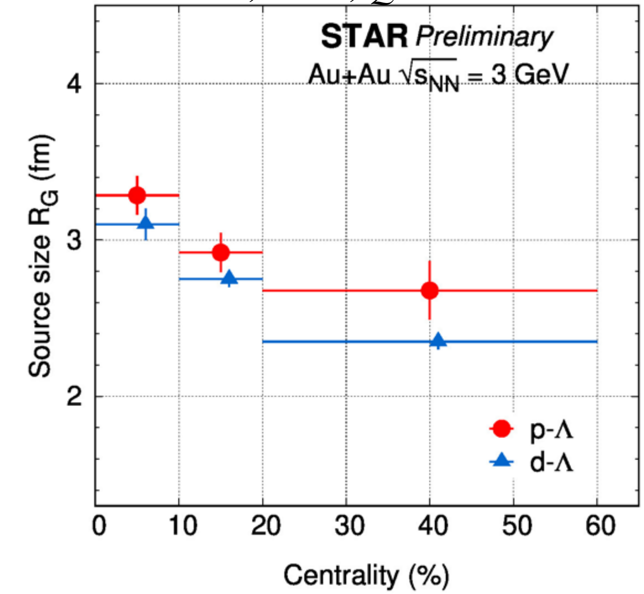

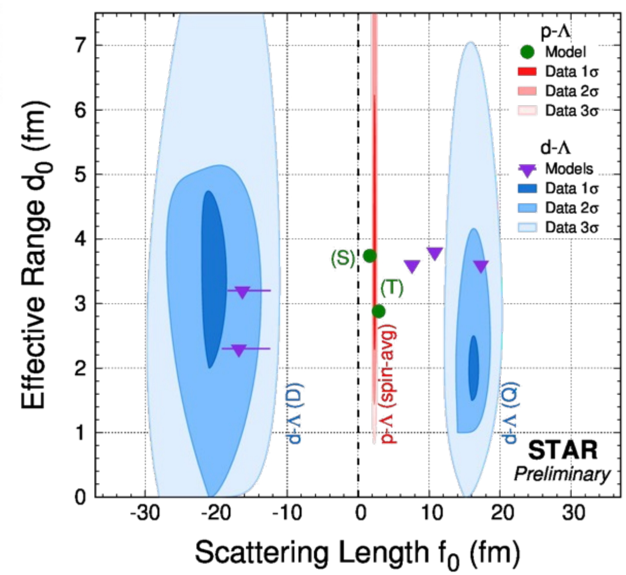

- There are difference between $\pi^+\pi^+$ and $\pi^-\pi^-$, which may be due to the mean field. Results follow the trends of STAR higher energy and HADES
- Separation of emission source from final state interactions in p-Λ and d-Λ correlation functions.

EM Probes - Thermal Dielectron

Y. Han, STAR, QM 2023

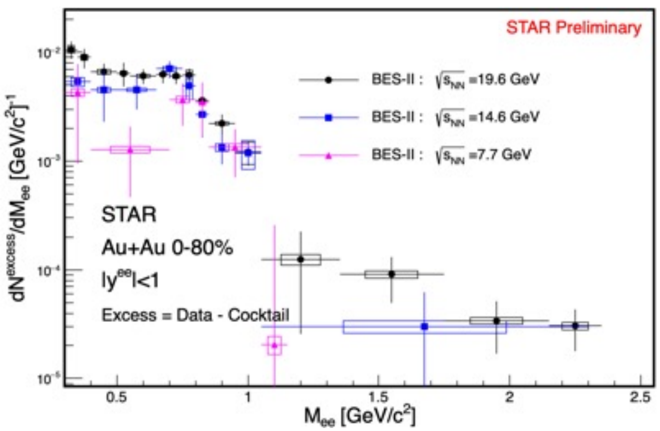

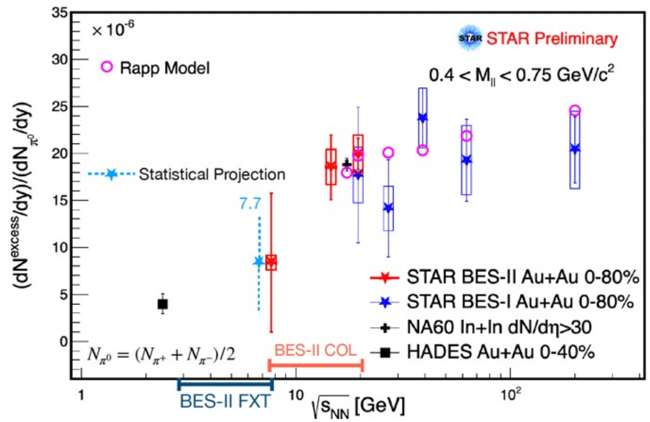

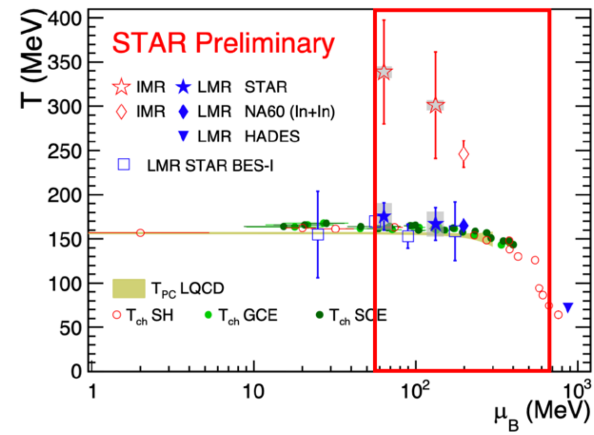

- Excess yield can be well described by in-medium ρ + QGP emission models

- Excess yield normalized by #of π^0
  - Consistent trend from BES-I to HADES (low to high μ_B)
  - Constrains medium interaction models

- T_{LMR} close to T_{ch} and T_{pc}, ρ meson dominantly emitted around phase transition, T_{IMR} higher than T_{ch} and T_{pc}, dielectron dominantly emitted from QGP phase

ϕ Global Spin Alignment

B. Xi, STAR, QM 2023

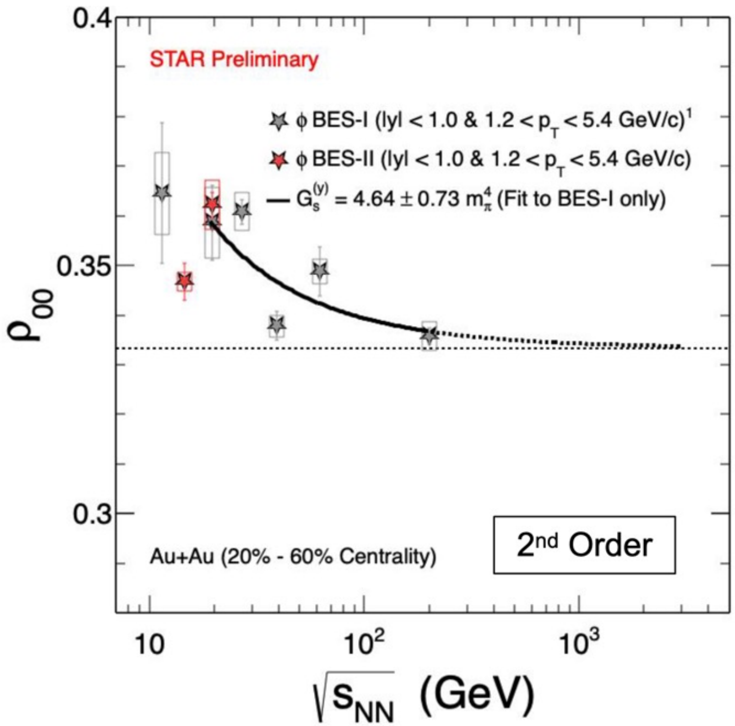

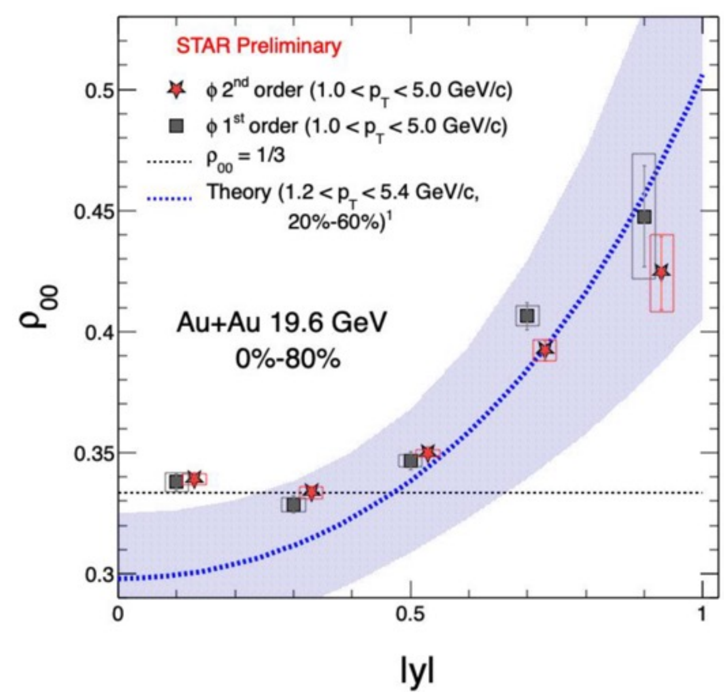

- Significant global spin alignment confirmed at BES-II 14.6 GeV and 19.6 GeV
- Rapidity dependence roughly agrees with theory invoking strong force field
  - larger fluctuation in the direction perpendicular to the motion direction

Nature 614 (2023) 7947.
X. L. Sheng, et al., arXiv:2308.14038 [nucl-th].

Summary

- STAR Beam Energy Scan program covers a wide range of topics and has collected a unique set of data on a variety of collision energies including fixed target data;

- All requested BES II data collected, providing 17 unique energies from 3-200 GeV with some overlapping collider and FXT energies;

- The properties of the medium behavior differently between high energies and low energies, stay tune for more interesting/precise results from BES-II;

Outlook

- High statistical data from BES-II and other facilities and experiments

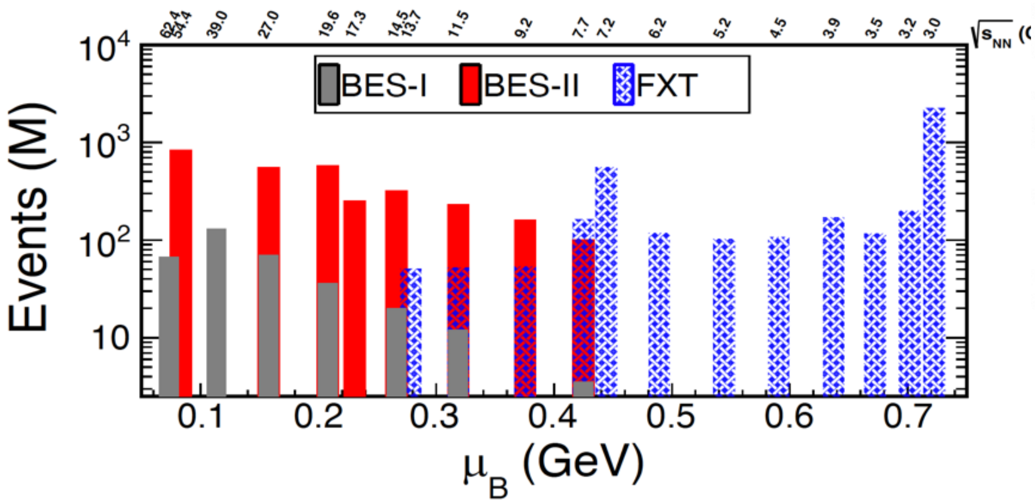

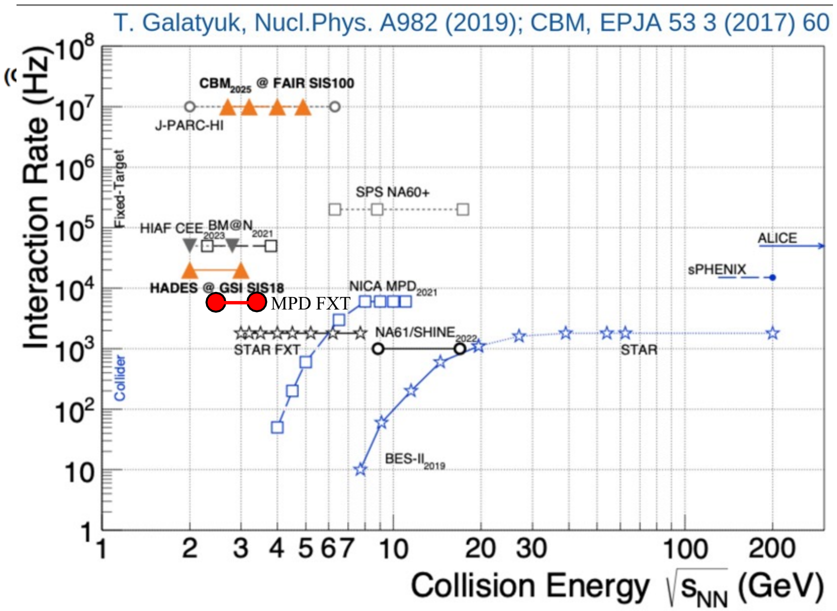

In this report:
Part of the STAR BES-II dataset are analyzed and reported, stay tune

中国科学院大学

University of Chinese Academy of Sciences

Thanks for Listening!